



## Optical, size and mass properties of mixed type aerosols in Greece and Romania as observed by synergy of lidar and sunphotometers in combination with model simulations: A case study



A. Papayannis <sup>a,\*</sup>, D. Nicolae <sup>b</sup>, P. Kokkalis <sup>a</sup>, I. Binietoglou <sup>b,c</sup>, C. Talianu <sup>b</sup>, L. Belegante <sup>b</sup>, G. Tsaknakis <sup>a</sup>, M.M. Cazacu <sup>d</sup>, I. Vetres <sup>e</sup>, L. Ilie <sup>f</sup>

<sup>a</sup> Laser Remote Sensing Unit, Physics Department, National Technical University of Athens, Greece

<sup>b</sup> National Institute of Research and Development for Optoelectronics, Magurele, Romania

<sup>c</sup> Istituto di Metodologie per l'Analisi Ambientale CNR-IMAA, Tito Scalo, Potenza, Italy

<sup>d</sup> Al.I.Cuza University of Iasi, Iasi, Romania

<sup>e</sup> Politehnica University of Timisoara, Timisoara, Romania

<sup>f</sup> Institute of Physics, University of Belgrade, Belgrade, Serbia

### HIGHLIGHTS

- We present coordinated lidar measurements in Greece and Romania.
- We measured optical, size and mass properties of mixed type aerosols.
- We intercompared aerosol mass concentrations from LIRIC and POLIPHON.

### ARTICLE INFO

#### Article history:

Received 7 April 2014

Received in revised form 14 July 2014

Accepted 26 August 2014

Available online xxxx

Editor: P. Kassomenos

#### Keywords:

Lidar

Aerosols

AERONET

Dust

LIRIC

POLIPHON

### ABSTRACT

A coordinated experimental campaign aiming to study the aerosol optical, size and mass properties was organized in September 2012, in selected sites in Greece and Romania. It was based on the synergy of lidar and sunphotometers. In this paper we focus on a specific campaign period (23–24 September), where mixed type aerosols (Saharan dust, biomass burning and continental) were confined from the Planetary Boundary Layer (PBL) up to 4–4.5 km height. Hourly mean linear depolarization and lidar ratio values were measured inside the dust layers, ranging from 13 to 29 and from 44 to 65 sr, respectively, depending on their mixing status and the corresponding air mass pathways over Greece and Romania. During this event the columnar Aerosol Optical Depth (AOD) values ranged from 0.13 to 0.26 at 532 nm. The Lidar/Radiometer Inversion Code (LIRIC) and the Polarization Lidar Photometer Networking (POLIPHON) codes were used and inter-compared with regards to the retrieved aerosol (fine and coarse spherical/spheroid) mass concentrations, showing that LIRIC generally overestimates the aerosol mass concentrations, in the case of spherical particles. For non-spherical particles the difference in the retrieved mass concentration profiles from these two codes remained smaller than  $\pm 20\%$ . POLIPHON retrievals showed that the non-spherical particles reached concentrations of the order of 100–140  $\mu\text{g}/\text{m}^3$  over Romania compared to 50–75  $\mu\text{g}/\text{m}^3$  over Greece. Finally, the Dust Regional Atmospheric Model (DREAM) model was used to simulate the dust concentrations over the South-Eastern Europe.

© 2014 Elsevier B.V. All rights reserved.

### 1. Introduction

Aerosols are important constituents of the atmosphere, influencing both the air quality and the Earth's climate. They scatter and absorb solar and terrestrial radiation (direct effect) and alter the physical, optical and lifetime properties of clouds and thus the precipitation formation (indirect effect), as they act as cloud condensation nuclei

(Ackermann and Chung, 1992; Seinfeld and Pandis, 1998; Lance et al., 2009; Cerully et al., 2011; Moore et al., 2013). However, the overall uncertainties in the radiative forcing effect of aerosols (anthropogenic and natural) remain still very high (Forster et al., 2007). These uncertainties can only be reduced by better quantifying the vertical and horizontal distribution of aerosols over the globe. Laser remote sensing (lidar) measurements of the vertical distribution of the aerosol optical, microphysical and mass properties can contribute to such quantification (Meloni et al., 2005; Heinold et al., 2011; Noh et al., 2012; Papayannis et al., 2012a; Kanitz et al., 2013; Reddy et al., 2013).

\* Corresponding author. Tel.: +30 210 7722992; fax: +30 210 7722928.

E-mail address: [apdlidar@central.ntua.gr](mailto:apdlidar@central.ntua.gr) (A. Papayannis).



**Fig. 1.** Map of the five monitoring sites (Athens, Oxylithos, Bucharest, Timisoara, Iasi) and the Xanthi (sun photometer) site, during the AGRO campaign.

Aerosols belong to two categories (Pandis et al., 1995): those of natural origin (marine, volcanic, desert, biogenic, etc.) and those of anthropogenic origin (biomass burning, fossil fuel burning, etc.). However, the main sources of aerosols are mainly the large deserts, the strong volcanic eruptions and the biomass-fossil fuels burning. As a result, there is a strong spatial and temporal variation of their vertical and horizontal distribution in the troposphere (Andreae and Crutzen, 1997; Prospero et al., 2002; Balin, 2004; Abbatt et al., 2006; Tunved et al., 2006; Yu et al., 2012; Lathem et al., 2013).

Since the establishment of the European Aerosol Research Lidar Network (EARLINET) in May 2000 (Bösenberg et al., 2003; Pappalardo et al., 2004), aerosol systematic observations combining active and passive remote sensors are performed over the European continent (Pérez et al., 2004; Mona et al., 2006; Papayannis et al., 2008;

Guerrero-Rascado et al., 2009; Pappalardo et al., 2010; Amiridis et al., 2013; Müller et al., 2013). In the South-Eastern (SE) European sector, systematic lidar measurements are performed in single stations in Greece, Bulgaria, Romania and recently in Cyprus, within the frame of EARLINET (Papayannis et al., 2008; Pappalardo et al., 2010; Mamouri et al., 2013; Nemuc et al., 2013; Nicolae et al., 2013).

Although the Balkan area and more specifically the Black and Aegean Seas are a cross road of several air pollutants (Lelieveld et al., 2002), no combined systematic aerosol profiling data (optical, micro-physical and mass properties) are available yet in Greece and Romania. Therefore, the level of understanding of the aerosol properties related to transport processes in SE Europe and especially over the Aegean and around the Black Sea, remains still quite low, despite some recently published data (e.g. Sciare et al., 2005; Koulouri et al., 2008; Kanakidou et al., 2011; Papayannis et al., 2012b; Theodosi et al., 2013).

To address these issues a coordinated experimental field campaign with synchronized aerosol observations was organized for the first time in Greece and Romania, at five selected stations (Fig. 1): Athens (Lat: 37.96°N, Lon: 23.78°E, 220 m above sea level (a.s.l.)), Oxylithos (Lat: 38.57°N, Lon: 24.13°E, 120 m a.s.l.), Bucharest (Lat: 44.35°N, Lon: 26.03°E, 93 m a.s.l.), Iasi (Lat: 47.17°N, Lon: 27.57°E, 200 m a.s.l.), and Timisoara (Lat: 45.73°N, Lon: 21.22°E, 102 m a.s.l.). The structure of this paper is as follows. Section 2 presents the methodology of the measurements and the models involved, while Section 3 shows the instrument description concerning the Greek and the Romanian infrastructure. Section 4 discusses a selected case study of Saharan dust

**Table 1**  
Selected instruments per site, used in the AGRO campaign of 15–29 September 2012.

| Site      |   |                |
|-----------|---|----------------|
| Athens    | $3b_{aer} + 2a_{aer}$ + aerosol Raman lidar                         | CIMEL (Xanthi) |
| Oxylithos | $1b_{aer} + 1\delta_p$ (532 nm) elastic lidar                       | CIMEL (Xanthi) |
| Timisoara | $1b_{aer}$ (532 nm) elastic lidar                                   | CIMEL          |
| Bucharest | $3b_{aer} + 2a_{aer} + 1\delta_p$ (532 nm)<br>+ aerosol Raman lidar | CIMEL          |
| Iasi      | $1b_{aer}$ (532 nm) elastic lidar                                   | CIMEL          |

particles advected and measured over the five sites, while in Section 5 we present our main conclusions.

## 2. Methodology

In order to investigate the vertical and spatial distribution of the aerosol optical, size and mass properties over our geographical area, related to long-range transport, an intensive campaign, called AGRO (including synergy of several instruments) was organized between 15 and 29 September 2012, simultaneously, in Greece and Romania at the aforementioned selected sites: Athens and Evia island on the Aegean Sea (Greece) and Bucharest, Iasi, and Timisoara (Romania). The AGRO campaign was organized to perform regular measurements within two sessions per day: (a) daytime: 06:00–09:00 UTC; (b) night time: 16:00 UTC–20:00 UTC. Weather and dust forecasts were issued each day prior to the measurements. During alerts, daily sessions were extended to: (a) daytime: 06:00 UTC–13:00 UTC; (b) night time: 16:00 UTC–21:00 UTC. For the lidar profiling, a total number of 282 hourly profiles were obtained, out of 412 scheduled. The difference is mainly due to rain and low clouds conditions, when lidar measurements were not possible. Range-corrected lidar time-series were computed and made freely available on line at: [http://physics.ntua.gr/~papayannis/gr\\_rom\\_2012/index.html](http://physics.ntua.gr/~papayannis/gr_rom_2012/index.html) (Greek stations), and <http://quicklooks.inoe.ro> (Romanian stations). These colour plots, describing the temporal evolution of the atmospheric structure and particle presence, were generally used to assess the height of the various aerosol layers.

During the AGRO campaign active and passive instruments were deployed (Table 1). Multi-wavelength Raman lidars were operated in Bucharest and Athens to provide quantitative vertical profiles of aerosol backscatter ( $b_{aer}$ ) and extinction ( $a_{aer}$ ) coefficients, as well as basic aerosol optical parameters (Ångström exponent, extinction-to-backscatter ratio (lidar ratio or S) and aerosol optical depth (AOD)). In all other sites, elastic backscatter lidars were operated.

In parallel to the lidar measurements, sun photometric measurements were performed over the experimental sites using selected

AERONET sun photometers operating in Greece and Romania (<http://aeronet.gsfc.nasa.gov>) (Holben et al., 1998), except over Athens and Oxylythos: in Athens the sun photometer was out of order between 12 and 28 September, while the Oxylythos site (a rural-marine site) is not equipped with a sun photometer. We then used the sun photometer data from the Xanthi station (Lat: 41.14°N, Long: 24.92°E, 54 m a.s.l.) (Fig. 1), as back-trajectory analysis (not shown) indicated that this station was affected by the same air masses as Athens and Oxylythos, for the period 23–24 September. Furthermore, the data provided by Xanthi station were found consistent with the ones provided by the nearby AERONET site of Thessaloniki; the other Greek AERONET site at Herakleion in Crete was not taken into account as it was located outside the overpassing of the sampled air masses.

The sun photometer data (level 1.5), given by the Cimel-318 instruments in Greece and Romania, were used to provide information about the columnar AOD, the aerosol size distribution (fine and coarse mode) (O'Neill et al., 2003), the aerosol microphysical properties and the Ångström exponent (AE). The inverted aerosol size distributions refer to aerosol radius ranging from  $0.01\text{ }\mu\text{m}$  to  $15\text{ }\mu\text{m}$ . According to Holben et al. (1998, 2006) and Smirnov et al. (2000), the expected accuracy for the AERONET inversions is of the order of  $\pm 0.03$  (cloud-screened data) for the AOD, of 15–25% for radius greater than  $0.5\text{ }\mu\text{m}$  and of 25–100% for radius less than  $0.5\text{ }\mu\text{m}$ . Detailed information on the pointing error and field-of-view and on the sensitivity of the aerosol retrieval to geometrical configuration of the Cimel-318 instrument is provided by Torres et al. (2013, 2014).

The Hybrid Single-Particle Lagrangian Integrated Trajectory (HYSPLIT) Lagrangian model (version 4.9) was used to compute 4-day three-dimensional air mass back-trajectories ending at different heights over our measuring sites, allowing estimating the aerosol source regions. HYSPLIT is a dispersion model that relies on meteorological data to drive the simulations. It uses 3-hourly archive meteorological data from the National Weather Service's National Centers for Environmental Prediction (NCEP) from the Global Data Assimilation Group (GDAS) as described in Draxler et al. (2009). The HYSPLIT model was

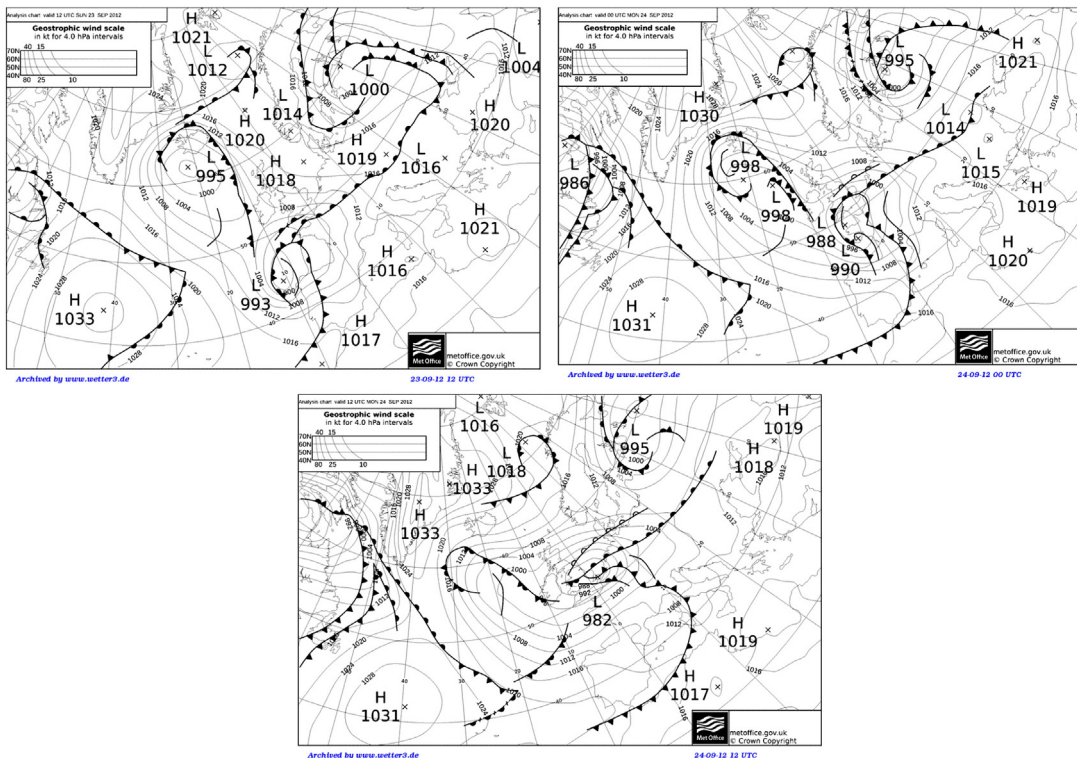


**Fig. 2.** Surface meteorological maps over Europe for 23 September at 12:00 UTC (upper left), 1 and 24 September at 00:00 UTC (upper right) and 12:00 UTC (lower part, middle), respectively.

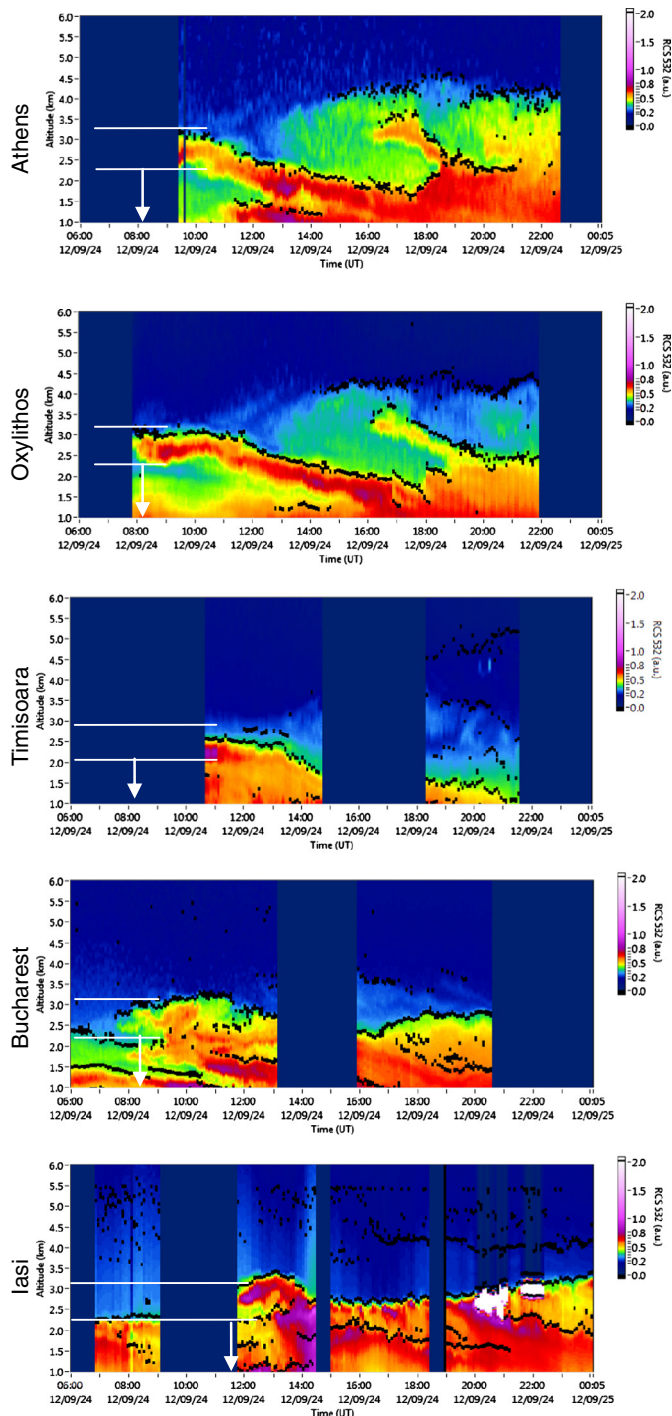


**Fig. 3.** Range-corrected lidar time-series at 532 nm, for the period from 24 September (06:00 UTC) to 25 September (00:05 UTC) 2012, showing the Saharan dust layer at 2.4–3.3 km height (white horizontal lines) and the estimated time of arrival (white vertical arrows) over Athens, Oxylythos, Timisoara, Bucharest and Lasi. Color codes are given in arbitrary units (A.U.), for each station. (For interpretation of the references to color in this figure legend, the reader is referred to the web version of this article.)

used during the campaign to provide indication of the air-mass origin and optimize the measurement schedule.

The FLEXPART particle dispersion model was used during the analysis phase to study in more detail the mixing of different aerosol types for selected cases. FLEXPART is a particle dispersion model (Stohl et al., 1998, 2005) that was used in the backward mode to identify the possible geographical regions (and with their subsequent aerosol load) that could contribute to the measured aerosol load

(Seibert and Frank, 2004). Like HYSPLIT, FLEXPART simulations are based on meteorological fields, but also take into account the turbulence and convection, by modeling them as random motions superimposed to the movement due to the wind field. Dry and wet deposition of particles was also considered. FLEXPART was driven by data provided by the National Centers for Environmental Prediction (NCEP), Climate Forecast System (CFS) (Saha et al., 2010) with a time resolution of 3 h and horizontal resolution of 1°. The model output was stored at a grid with horizontal resolution of  $0.2^\circ \times 0.2^\circ$  and 10 vertical levels with 1 km range resolution.

An additional model was used to provide the horizontal and vertical cross sections of the dust concentration along Athens–Oxylythos–Xanthi–Bucharest. The simulated vertical dust profiles were evaluated by a version of the Dust Regional Atmospheric Model (DREAM) (Nickovic et al., 2001; Nickovic, 2005) embedded into the NCEP/NMME non-hydrostatic atmospheric model (Janjic et al., 2011). The model uses 8 particle size bins within the 0.1–10 microns radius range, and it is utilized for operational dust forecast at the South East European Virtual Climate Change Center (SEEVCCC; <http://www.seevccc.rs>), hosted by the Serbian Meteorological Service. The model includes an assimilation of satellite MODIS/AOD data (Pejanovic et al., 2010). The model horizontal resolution is 1/5° ( $\sim 30$  km) and has 28 vertical levels. Its domain covers the Saharan and Middle East dust sources, as well as a large part of the European continent.

Furthermore, the Lidar/Radiometer Inversion Code (LIRIC), which uses the lidar and sunphotometer data, was used to derive particle volume and mass concentration profiles for fine-mode and coarse-mode particles (Kokkalis et al., 2013; Tsekeri et al., 2013; Wagner et al., 2013). Four elastic lidar signals, including depolarization (355 nm, 532 nm with cross and parallel polarization, and 1064 nm), and AERONET retrievals were taken into account to derive aerosols optical and microphysical vertical profiles that are best fitted to the column-integrated values. Moreover, when cross-polarized lidar measurements at 532 nm are available, LIRIC has the capability to differentiate the coarse mode concentration into spherical and non-spherical components (Chaijkovsky et al., 2012).

Finally, we used the POLIPHON algorithm to estimate the vertical profile of the mass concentration of the dust and non-dust component of the atmospheric aerosols (Ansman et al., 2012). This algorithm is based on the synergy of depolarization lidar and sun photometric measurements. The basic idea of this algorithm is to make use of the depolarization lidar measurements to separate the contribution of dust and non-dust aerosol types to the measured aerosol backscatter coefficient profiles. Then, the mass concentrations of the dust components are calculated by making use of their known properties: depolarization ratio, extinction-to-backscatter ratio, mass density and volume-to-extinction ratio estimated from the sun photometer measurements. In contrast to LIRIC, the sun photometer measurements are used to derive only intensive aerosol properties and thus reasonable results can be derived even if the lidar and sun photometer measurements are not strictly collocated and simultaneous; this is especially true for the Saharan dust, as the volume-to-extinction ratio has been found to be relatively stable for specific dust events (e.g. Ansman et al., 2012).

### 3. Instrument description

#### 3.1. Greek stations infrastructure

##### 3.1.1. Athens site

The Athens (Greece) site belongs to the Laser Remote Sensing Unit of the National Technical University of Athens (NTUA) and is located in the Greater Athens area (Fig. 1). The NTUA lidar system (EOLE) is based on a pulsed Nd:YAG laser, emitting simultaneously at 355, 532, and 1064 nm, at 10 Hz repetition rate. The full overlap of the system is obtained at 0.5 km (at 532 nm) and at 0.7 km (at 1064 nm) above

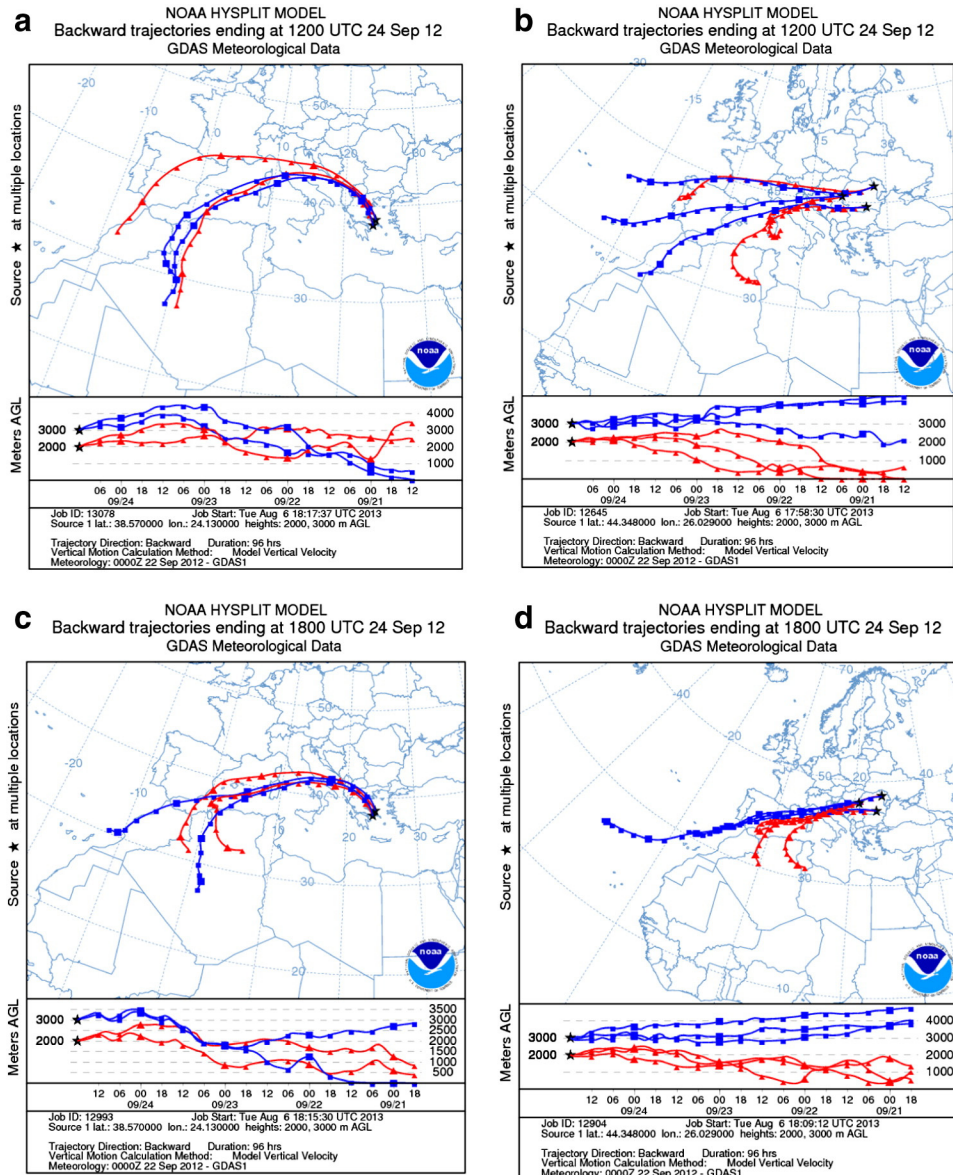


**Fig. 4.** Air mass back trajectories of air masses arriving on 24 September 2012, at 12:00 UTC over: (a) the Greek stations and (b) the Romanian stations, at 2 km and 3 km altitude height and at 18:00 UTC over: (c) the Greek stations and (d) the Romanian stations, at 2 km and 3 km altitude height.

ground, according to the detected wavelengths. A 300 mm diameter optical Cassegrainian telescope collects the elastically (355–532–1064 nm) and Raman (from N<sub>2</sub> at 387 nm and 607 nm and from H<sub>2</sub>O at 407 nm) backscattered lidar signals. A high grade all-fused silica optical fiber is used to transfer the lidar signals to an advanced 6-wavelength spectrometer, which is equipped with achromatic collimating lenses, dichroic beam splitters, as well as doublets, eye pieces and narrow interference filters (IFF) placed in front of the detectors (Photomultiplier tubes-PMTs at 355–387–407–532–607 nm and an Avalanche Photo Diode-APD at 1064 nm). EOLE is equipped with LICEL GmbH (Germany) transient recorders (model TR 40-120), with 20 MHz sampling rate (7.5 m range resolution) and 12-bit digital-to-analog converters. Full details of the NTUA Raman lidar system are provided in Kokkalis et al. (2012).

The lidar signals detected at 355, 387, 532, 607 and 1064 nm, were used to derive the aerosol backscatter (at 355, 532 and 1064 nm) and extinction (at 355 and 532 nm) coefficients, as well as the lidar ratio ( $S = a_{aer}/b_{aer}$ ), and Ångström exponent (AE). The NTUA lidar system, being part of EARLINET, has been quality-assured through direct inter-

comparisons, both at hardware (Matthias et al., 2004) and algorithm levels (Böckmann et al., 2004; Pappalardo et al., 2004). During daytime, we use the Klett technique (Klett, 1981, 1985) using as input a constant S value (constrained to the mean AOD value obtained from a nearby sunphotometer, see for e.g. Landulfo et al., 2005) to retrieve the  $b_{aer}$  values with an average uncertainty (due to both statistical and systematic errors) of the order of 20–30% (Bösenberg et al., 2003).

When nearby sunphotometry data are missing (as in the case of Greece for the period under study), we then use the most probable S values, related to the air masses sampled (e.g. urban, maritime, biomass burning, etc.), which are provided by long-term Raman lidar measurements over Greece (e.g. Papayannis et al., 2008; Giannakaki et al., 2010). During nighttime we use the Raman technique (Ansmann et al., 1992) to retrieve the  $a_{aer}$  and  $b_{aer}$  vertical profiles with systematic uncertainties of ~5–15% and ~10–25%, respectively (Ansmann et al., 1992; Mattis et al., 2002). Thus, the corresponding vertical profile of S is calculated with a corresponding systematic uncertainty of the order of 5–10%. The mean uncertainty determined for Ångström exponents used in this study is  $\pm 0.3$ .



**Fig. 5.** Fire hotspots detected by MODIS from 22 to 24 September 2012. Data provided by FIRMS/NASA.

### 3.1.2. Oxylythos site

The Oxylythos site is located at 3 km distance from the Aegean Sea (Fig. 1) near the top of a hill facing the sea from its north-eastern side. In this location, the NTUA mobile lidar system (AIAS) was operated during the field campaign. AIAS is a truck-mounted 532 nm commercial depolarization lidar system manufactured by Raymetrics S.A. (Greece). AIAS is based on a pulsed Nd:YAG laser, emitting only at 532 nm, at 10 Hz repetition rate. The full overlap of the system is obtained already at 0.3 km above ground level. A 200 mm diameter optical Cassegrainian telescope collects the elastically backscattered lidar signal at 532 nm, at two different polarizations: vertical (*s*-cross) and parallel (*p*-parallel) one. AIAS is equipped with LICEL GmbH (Germany) transient recorders (model TR 40-120), with a 20 MHz sampling rate (7.5 m range resolution) and 12-bit digital-to-analog converters.

AIAS is able to provide the aerosol linear depolarization ratio ( $\delta_p$ ) in the troposphere, thus evaluating the form of the probed aerosols (spherical/non spherical particles). Its calibration is based on the  $\pm 45^\circ$  ( $\pm 0.2^\circ$ ) methodology described in Freudenthaler et al. (2009). The corresponding uncertainty in the retrieval of the aerosol linear depolarization ratio is of the order of 15%. As mentioned previously, as no sunphotometer data were available for Athens and Oxylythos, we used the Cimel data from the AERONET site in Xanthi (located 373 km north-eastern of Athens) (Fig. 1).

### 3.2. Romanian stations infrastructure

#### 3.2.1. Bucharest site

The Bucharest site is located in the Magurele region in the south-western part of the capital city of Romania (Fig. 1). At this site, the monitoring of local and long-range transported aerosols is regularly performed using a multi-wavelength Raman lidar system (RALI) manufactured by Raymetrics S.A. (Greece). This station is part of EARLINET since 2005. RALI is a bi-axial system with combined elastic and Raman detection (Nemuc et al., 2013). The emission system is based on a pulsed Nd:YAG laser that emits at 355, 532, 1064 nm and the reception system is based on a Cassegrainian telescope with a 400 mm diameter that collects the radiation at 1064 nm, 532 nm (*p*-parallel), 532 nm (*s*-cross), 607 nm, 387 nm, 355 nm and 408 nm. The range of measurements is limited in the lower part of the bi-axial lidar system by the incomplete overlap of the laser beam to

the telescope's field of view. The detection range can be extended dynamically from 750 m (full overlap) up to 15 km, by using combined analog and photon counting detection. Parallel and cross 532 nm channels provide calibrated depolarisation ratios, based on a  $\pm 45^\circ$  calibration module (Freudenthaler et al., 2009). The RALI acquisition system is equipped with LICEL GmbH (Germany) transient recorders (model TR 40-120), with a 40 MHz sampling rate (3.75 m range resolution) and 12-bit digital-to-analog converters.

The RALI system is used to study the aerosol optical, size and microphysical properties (Nicolae et al., 2008, 2013; Nemuc et al., 2013). Vertical profiles of aerosol backscatter and extinction coefficients, lidar ratios at 532 and 355 nm, as well as Ångström exponent are calculated from lidar range-corrected signals, using combined Raman-Mie inversion (Ansmann et al., 1992) during nighttime measurements, with the same accuracy as the EOLE data. Under daytime conditions, where the atmospheric background radiation is too high, RALI cannot use the Raman-Mie inversion technique; therefore, only the aerosol backscatter coefficients can be retrieved using the Klett method (Klett, 1981, 1985) with an uncertainty of 20–30% (Bösenberg et al., 2003). The uncertainty on the retrieved particle linear depolarization ratio is about 15%.

Layer mean values of the effective radius, single-scattering albedo and complex refractive index are calculated by the inversion methodology described by Müller et al. (1999) with statistical uncertainties less than 10%. The method uses as input aerosol backscatter coefficients at 355, 532 and 1064 nm and aerosol extinction coefficients at 355 and 532 nm. Lidar ratios are provided with an accuracy of 10–15%. The mean uncertainty determined for Ångström exponents used in this study is  $\pm 0.3$ .

As previously mentioned, an AERONET sun photometer is also used to measure column integrated aerosol optical properties, and to retrieve the average column Ångström exponents, size distribution, single scattering albedo (SSA) and other optical and microphysical parameters (see for example Dubovik et al., 2000).

#### 3.2.2. Iasi and Timisoara sites

The Romanian sites Iasi and Timisoara are located in the north-eastern part and western part of Romania, respectively (Fig. 1). At each of these locations, an elastic backscatter lidar system was operated during the field campaign. These systems are based on a pulsed Nd:YAG laser, emitting at 532 nm, with 30 Hz repetition rate. The reception systems are based on a Newtonian telescope with a 400 mm diameter

having a full overlap of the order of 750 m. Both sites are equipped with optical particle counters and meteorological stations. Sun photometers in Magurele, Timisoara and Iasi, which are part of AERONET, performed aerosol measurements at eight spectral bands (340, 380, 440, 500, 670, 870, 940 and 1020 nm).

#### 4. Case study of 23–24 September 2012

Out of the total period of the AGRO campaign (15–29 September 2012), we selected to focus on the spatial distribution of the aerosol properties, in four dimensions (2 dimensional horizontal, vertical and temporal scales) during a special event of Saharan dust transported from Northern Africa over the Balkans area. This Saharan dust was captured during the AGRO campaign; starting on the night of 23 September in Athens, arriving in the early morning hours at Oxylythos and Timisoara and reaching Bucharest and Iasi before noon on 24 September.

##### 4.1. Meteorological synoptic analysis

We will shortly present now the meteorological synoptic analysis for the period between 23 September (12:00 UTC) and 24 September (12:00 UTC) (Fig. 2) based on meteorological maps at surface level. On

23 September (12:00 UTC) an extended low system (995 hPa) was located over the Atlantic Ocean, west of France and the north-west from the Iberian Peninsula (Fig. 2, upper left). On the other hand, an extended high pressure system (1015–1020 hPa) was located over Italy and the Balkan region and moves eastward. Later, on 24 September at 00:00 and 12:00 UTC (Fig. 2, upper right and lower middle, respectively) the 990 hPa low moves slightly eastward, while the Balkans region remains always under a high pressure system. Under these synoptic conditions, air masses from north-eastern Africa were advected over the Mediterranean Sea toward the Balkans region. This will be further corroborated by the FLEXPART simulations.

##### 4.2. Experimental data

At first we will present an overview of the vertical structure of the aerosol load in the lower troposphere, from 24 September (06:00 UTC) to 25 September (00:05 UTC). Thus, in Fig. 3 we present the range-corrected lidar signals at 532 nm, as time-series versus height above mean sea level height, for the above mentioned period, taking into account only the available lidar measurements for each station (Athens, Oxylythos, Timisoara, Bucharest and Iasi) in the altitude range 1 to 6 km height a.s.l. In all these color plots (shown in arbitrary units-A.U. for each sampling station) an intense aerosol layer is sampled

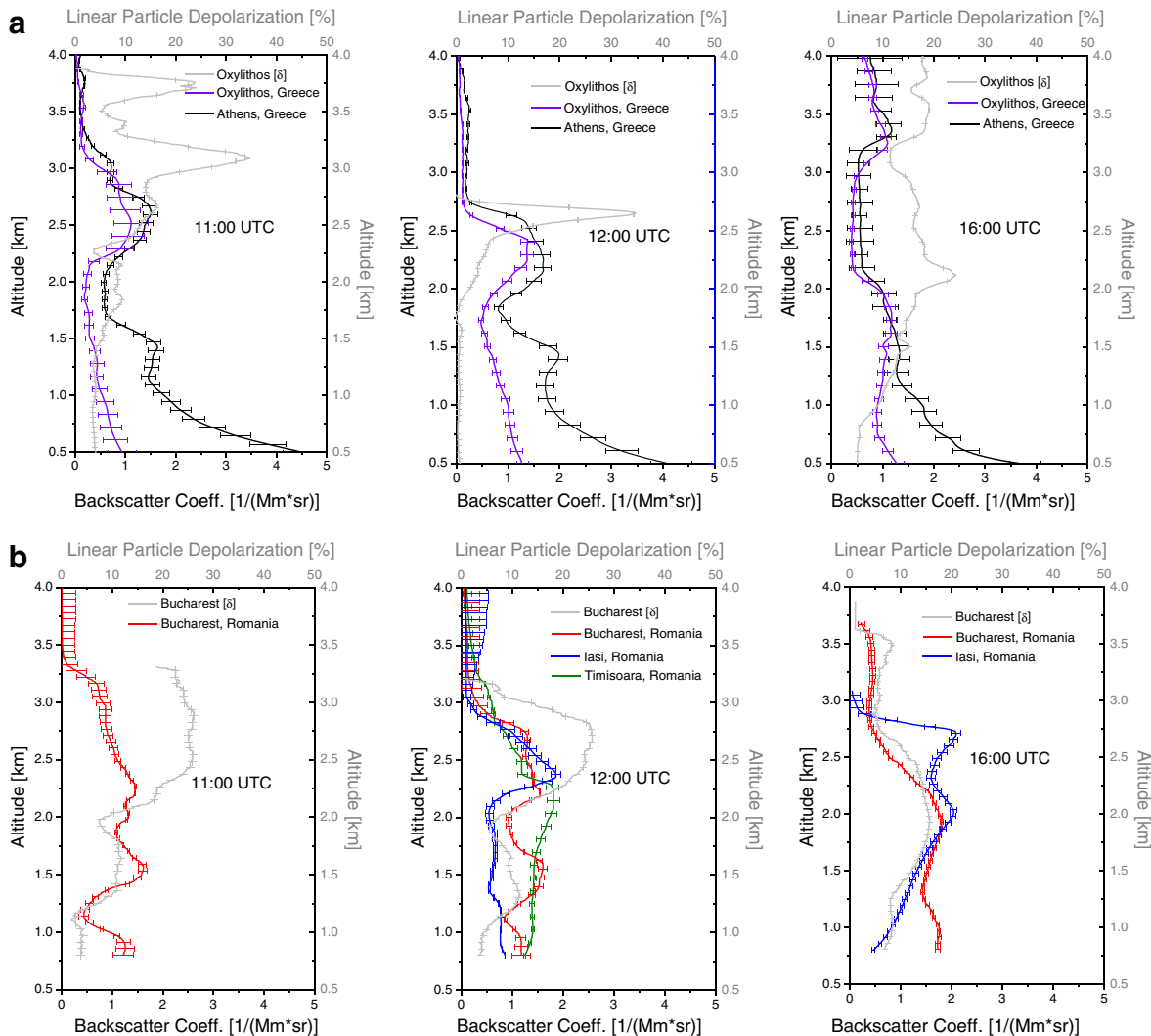


**Fig. 6.** a. Aerosol backscatter coefficient (violet and black) and linear particle depolarization (gray line) profiles at 532 nm over Greece on 24 September 2012 at 11:00 UTC (left), 12:00 UTC (middle) and 16:00 UTC (right). b. Aerosol backscatter coefficient (blue, green and red lines) and linear particle depolarization (gray line) profiles at 532 nm over Romania on 24 September 2012 at 11:00 UTC (left), 12:00 UTC (middle) and 16:00 UTC (right). (For interpretation of the references to color in this figure legend, the reader is referred to the web version of this article.)

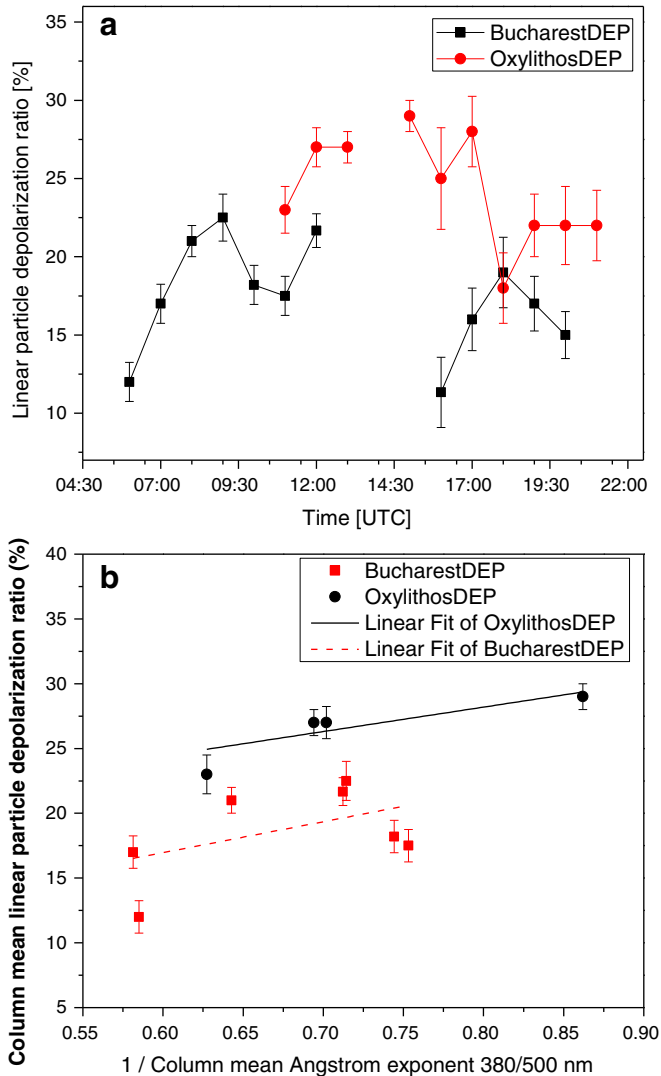


**Fig. 7.** a. 12-hour temporal evolution of the 1-hour average aerosol linear depolarization ratio at 532 nm (error bars are calculated as the standard deviation within the layers) obtained by lidar over Bucharest and Oxylythos (in %) on 24 September 2012, between 1.4 and 4 km height (from 05:30 to 21:00 UTC). b. Correlation of the column mean linear particle depolarization ratio measured by lidar at 532 nm, and the inverse of the column mean Ångström exponent (380/500 nm) retrieved by AERONET for Bucharest (Bucharest data) and Oxylythos (Xanthi data) on 24 September 2012.

between 1.5 and 3–3.2 km height a.s.l. The white horizontal lines (in Fig. 3) between 2.4 and 3.3 km height a.s.l., mark the position of the intense relevant aerosol layers. These layers were identified as containing dust particles, according to the Hysplit/FLEXPART codes; the air mass back-trajectories ending on 24 September at 2 and 3 km height at 12:00 UTC over the two Greek (Fig. 4a) and the three Romanian stations (Fig. 4b) and at 18:00 UTC, respectively (Fig. 4c and d), originated

from the Saharan region (in northern Africa), four days earlier. On the other hand the white vertical arrows in Fig. 3 mark the estimated time of the arrival of the Saharan dust plume over each sampling station.

Additionally, we mention here that, based on MODIS/Firemap observations for the period 22–24 September (Giglio et al., 2003), the northern Africa, the southern Italy (Sicily island) and the border area between Bulgaria and Romania, were also strong sources of smoke particles, due to intense biomass burning activity, during the studied period (cf. Fig. 5).

Furthermore, we will present the aerosol backscatter and depolarization profiles retrieved from lidar data over the two Greek sites (Athens and Oxylythos) and the three Romanian sites (Bucharest, Iasi, Timisoara) for 24 September (Fig. 6a and b). More precisely, at 11:00 UTC we observe in Fig. 6a (left panel) the existence of a strong aerosol layer over both sites (Athens and Oxylythos) from about 2.25 up to 3.2 km height. This layer shows strong linear particle depolarization values (over Oxylythos) of about 15%, with peaks of 35% around 3 km height. One hour later at 12:00 UTC (Fig. 6a, middle panel) we observe a subsidence of the aerosol layer down to 1.7–2.7 km with a high linear depolarization peak (~35%) around 2.6 km. Four hours later at 16:00 UTC (Fig. 6a, right panel) we observed a re-enhancement and rearrangement of the aerosol layers in the height range from 1 to 4 km, while the aerosol linear depolarization values dropped down to 10–25%, which is comparable with the values provided by CALIPSO (not shown) sampling nearly the same air masses along its overpass over Athens and Bucharest (at a distance less than 100 km for both sites, not shown here) (Winker et al., 2009; Mamouri et al., 2009).

Concerning the lower heights (below 1.7 km), between 11:00 and 12:00 UTC, we notice an enhancement of the  $b_{aer}$  values over Athens (by a factor of the order of 3 compared to the ones over Oxylythos), with a distinct aerosol layer over Athens around 1.45 km height (Fig. 6a, left and middle panels). Finally, at 16:00 UTC (Fig. 6a, right panel), the aerosol load is again enhanced between 1 and 2 km height, with aerosol linear depolarization values of the order of 5–10% over Oxylythos. Therefore, in general over Greece, the dust load is mainly confined between 1.5 and 3.2 km height, with aerosol linear depolarization values on the order of 10 and 35%, in the case of the Oxylythos site. The differences observed between Athens and Oxylythos below 1.5 km are probably due to the local aerosol contribution inside the PBL over Athens.

The lidar derived aerosol backscatter vertical profiles on 24 September over Bucharest, Iasi and Timisoara together with the linear particle depolarization ratio profiles over Bucharest, are shown at 11:00 and 12:00 UTC (Fig. 6b left and middle panels). Two aerosol layers are visible over Bucharest (1.1–1.8 km and 2–3.2 km), and one high-load aerosol layer over Iasi and Timisoara (between 2 and 3 km). The layer detected below 2 km in Bucharest shows a significantly lower particle depolarization ratio (<10%) than the layer above. The high depolarizing layer arriving at 2–3 km height over all Romanian stations (Fig. 6b at 11:00 UTC and 12:00 UTC, left and middle panels) is slowly descending and is mixed with local aerosol after sunset (Fig. 6b, right panel at 16:00 UTC).

The mean values of the linear particle depolarization were calculated in the layers between 1.4 and 4 km height (at 532 nm on 24 September from 05:30 to 21:00 UTC) for Bucharest and Oxylythos stations, where the lidar profiles are comparable (cf. Fig. 7a; error bars are calculated as the standard deviation within the layers). The aerosol layer selected shows aerosol linear depolarization values (over Bucharest) of about 25% at 11:00 UTC and 12:00 UTC (cf. Fig. 6b, left and middle panels) and a lower value (around 15%) at 16:00 UTC (cf. Fig. 6b, right panel). In general, higher linear depolarization ratio values were measured in Oxylythos (18–30%) than in Bucharest (12–23%) (cf. Fig. 7a). This difference is possibly related to the accentuated mixing of non-spherical particles with continental polluted aerosols and/or biomass burning particles (as previously mentioned) during longer and different air mass transport paths to Bucharest (cf. Fig. 4b, d).

**Table 2a**

Hourly mean values of the aerosol optical properties (aerosol depolarization ratio) derived from lidar measurements in Oxylythos and Bucharest on 23 and 24 September (11:00 to 21:00 UTC) in the range 1.4–4 km height.

| Site      | Date/hour | Aerosol optical properties<br>(aerosol depolarization ratio, %) |        |        |        |        |        |
|-----------|-----------|---|--------|--------|--------|--------|--------|
|           |           | 11:00   | 13:00  | 15:00  | 17:00  | 19:00  | 21:00  |
| Oxylythos | 23.09     | 5 ± 1   | 2 ± 0  | 5 ± 1  | 2 ± 0  | 2 ± 0  | 5 ± 1  |
|           | 24.09     | 23 ± 3  | 27 ± 4 | 29 ± 4 | 28 ± 4 | 22 ± 3 | 22 ± 3 |
| Bucharest | 23.09     | 9 ± 3   | N/A    | 7 ± 3  | 5 ± 3  | 11 ± 4 | 10 ± 4 |
|           | 24.09     | 17 ± 5  | 22 ± 5 | 13 ± 3 | 16 ± 3 | 17 ± 3 | 15 ± 3 |

**Table 2b**

Height ranges of aerosol layers and aerosol type observed on 24 September (11:00, 12:00 and 16:00 UTC) for all stations.

| Site      | Date/hour (UTC) | Altitude of aerosol layers (km) |         |         | Aerosol type                  |
|-----------|-----------------|---------------------------------|---------|---------|-------------------------------|
|           |                 | 11:00                           | 12:00   | 16:00   |                               |
| Athens    | 24.09           | 1.0–1.7                         | 1.0–1.7 | 1.0–2.0 | Industrial/smoke              |
|           |                 | 2.0–3.0                         | 1.7–2.7 | 3.0–4.5 | Mixed dust                    |
|           |                 | 2.3–3.5                         | 1.7–2.7 | 0.8–2.1 | Mixed marine with continental |
| Oxylithos | 24.09           |                                 |         | 3.0–4.5 | Mixed dust                    |
| Bucharest | 24.09           | 1.1–1.8                         | 1.0–1.8 | 1.5–2.7 | Industrial/smoke              |
|           |                 | 2.0–3.2                         | 2.0–3.0 |         | Mixed dust                    |
|           |                 |                                 |         |         | Mixed dust                    |
| Iasi      | 24.09           | N/A                             | 2.0–3.0 | 1.5–3.0 | Mixed dust                    |
| Timisoara | 24.09           | N/A                             | 2.0–3.0 | N/A     | Mixed dust                    |

This is also reflected in the aerosol depolarization ratios measured at these two sites from 11:00 to 21:00 UTC, before and after the arrival of the dust event (23 and 24 September) (cf. Fig. 7a). Indeed, before the arrival of the bulk of the dust particles the aerosol depolarization ratios were lower than 11%, while during the event they raised up to 13–29%.

Fig. 7b shows the relation between the particle's asphericity (linear particle depolarization ratio at 532 nm from lidar data) and their size (Ångström exponent at 380/500 nm from sun photometer data) as measured above Romania (Bucharest) and Greece (Xanthi) on 24 September. For both locations, an increase of the particle size (Ångström exponents from 1.8 to 1.1) corresponds to an increase of the asphericity (e.g. over Bucharest: from 12 to 22% in the column mean linear particle depolarization ratio in Fig. 7b), which suggests that the coarse mode is mostly represented by mineral dust. A slightly lower slope of the linear fit (0.19 versus 0.23) is visible for Oxylithos (Xanthi data), which could be related to an eventual mixture of mainly dust aerosols [as over Xanthi the columnar linear particle depolarization is also quite high: 23–30% (cf. Fig. 7b) and the aerosol fine mode fraction is quite low (~0.45, cf. Fig. 9a), which are both typical for dust particles] with other type of aerosols, leading to coarse particles with a lower slope in asphericity. Similar values for Ångström exponents determined from multi-wavelength lidar observations were presented in Fig. 18, page 157, Chapter VI "Optical properties of Saharan dust" of the PhD thesis of I. Balin (Balin, 2004). In Table 2a we summarize the aerosol optical properties (aerosol depolarization ratio in %) derived from lidar

measurements in Oxylithos and Bucharest on 23 and 24 September (11:00 to 21:00 UTC) in the range 1.4–4 km height.

In Table 2b we present the height ranges of aerosol layers and type observed on 24 September at 11:00, 12:00 and 16:00 UTC for all stations. The criterion of height range aerosol layer selection is based on the gradient method, proposed initially by Endlich et al. (1979) and extensively used recently by Di Giuseppe et al. (2011), Comerón et al. (2013), and Angelini and Gobbi (2014). In Table 2b we can also see the different types of mixed aerosol particles of different origin (industrial, smoke, dust, marine, continental, etc.) based on the HYSPLIT calculations.

We also compared the temporal evolution of the mean hourly lidar ratio values (in sr) at 532 nm, measured over Athens and Bucharest, for 24 September (Fig. 8, right vertical axis and Table 2c) and obtained for altitudes between 1.4 and 4 km, where the dust layers have been determined (Table 2b). In general, similar values of S ranging between 36 and 52 sr were found at both stations. Minimum S values at 532 nm were measured over Athens (45 sr) (Fig. 8, right vertical axis, gray line) around 20:00 UTC and over Bucharest around 18:00 UTC (36 sr) (Fig. 8, right vertical axis, orange line). The latter corresponds to maximum particle depolarization values (19%) over Bucharest (Fig. 8, left vertical axis, red line and right vertical axis, orange line), and consequently to a higher proportion of mineral dust in the aerosol mixture. However, these generally low S values indicate a possible presence of marine particles mixed with dust, as will be discussed later. On the other hand, the high S values, measured after 19:00 UTC, indicate an increase of the mixing of dust particles with continental polluted aerosols, both over Greece and Romania, as hinted by the CALIPSO satellite (data of 24 and 25 September, not shown) and as similarly reported by Mattis et al. (2002) and Mona et al. (2012). Indeed, the CALIPSO overpasses related to Iasi (at a 19 km distance, on 24 September 2012 at 11:15 UTC) and Timisoara (at a distance 32 km on 25 September 2012, at 00:50 UTC) show the existence of mixed dust aerosol layers between 2.5 and 4 km height (not shown).

Indeed, according to HYSPLIT, as mentioned previously (Fig. 4 a to d), on 24 September at 18:00 UTC, the air masses arriving at 2 km height over the 5 sampling stations are all coming from the same region of northern-northern-western Africa, and from very low altitudes (<1 km). As a consequence, these air masses were rich in mineral dust particles, on their way to the different stations in Greece and Romania.

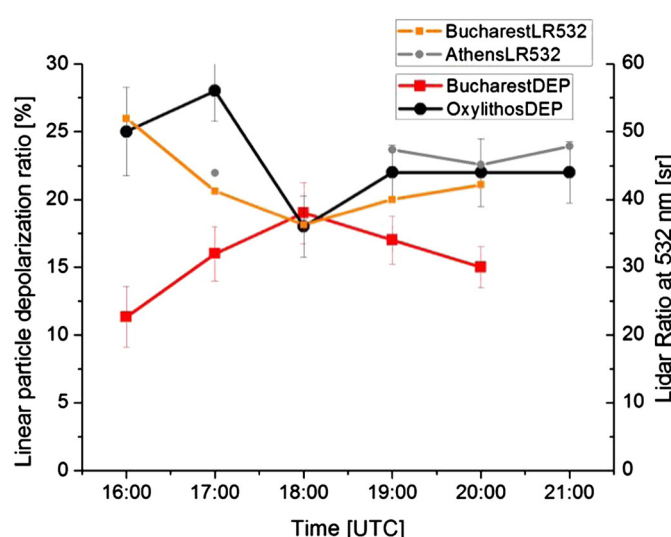


Fig. 8. Hourly mean lidar ratios obtained at 532 nm by Raman lidar (right vertical axis: gray and orange lines) over Bucharest and Athens on 24 September 2012, and the corresponding mean linear particle depolarization ratios (in %) (left vertical axis: red and black lines). (For interpretation of the references to color in this figure legend, the reader is referred to the web version of this article.)

**Table 2c**

Hourly mean values of the aerosol optical properties (lidar ratio) derived from lidar measurements in Athens and Bucharest on 23 and 24 September (11:00 to 21:00 UTC) in the height range 1.4–4 km.

| Site      | Date/hour | Aerosol optical properties (lidar ratio, in sr) |        |        |        |        |        |  |
|-----------|-----------|---|--------|--------|--------|--------|--------|--|
|           |           | 16:00   | 17:00  | 18:00  | 19:00  | 20:00  | 21:00  |  |
| Athens    | 23.09     | N/A   | 52 ± 5 | N/A    | 57 ± 5 | 58 ± 5 | 56 ± 5 |  |
|           | 24.09     | N/A   | 44 ± 4 | N/A    | 47 ± 5 | 45 ± 5 | 48 ± 5 |  |
| Bucharest | 23.09     | 65 ± 4  | 57 ± 5 | 55 ± 5 | 51 ± 3 | 53 ± 4 | N/A    |  |
|           | 24.09     | 52 ± 4  | 41 ± 5 | 36 ± 5 | 40 ± 5 | 42 ± 4 | N/A    |  |

**Table 3**

Daily mean values of the Angstrom Exponent (AE) (440/870 nm) and aerosol optical depth (AOD) derived from the sun photometers at 500 nm on 23 and 24 September.

| Station   | Date  | AE (440/870 nm) | AOD (500 nm)  |
|-----------|-------|-----------------|---|
| Xanthi    | 23.09 | 1.272           | Decreasing from 23 to 24 Sep. at all stations           |
|           | 24.09 | 0.778           | (due to the arrival of large mineral dust particles)    |
|           | Var.  | ↙               | ↗   |
| Timisoara | 23.09 | 1.519           | Increasing with distance from the source                |
|           | 24.09 | 1.193           | (due to mixing with small size polluted/smoke aerosols) |
|           | Var.  | ↘               | ↗   |
| Bucharest | 23.09 | 1.773           |   |
|           | 24.09 | 1.288           |   |
|           | Var.  | ↘               | ↗   |
| Iasi      | 23.09 | 1.774           |   |
|           | 24.09 | 1.644           |   |
|           | Var.  | →               | ↗   |

From these plots it is visible that the dust particles arrived first at Greek stations and Timisoara, and then at Bucharest and Iasi stations, which is consistent with our lidar profiling measurements (Fig. 6a and b),

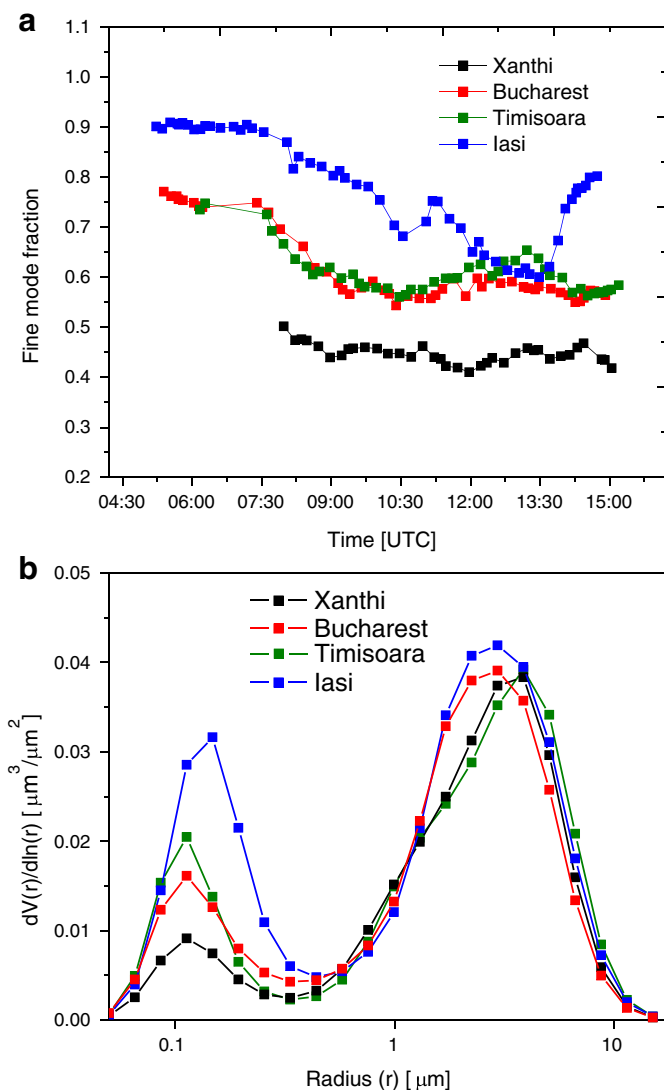


**Fig. 9.** a. Temporal variation of the aerosol fine mode fraction derived from sun photometer measurements over Greece: Xanthi (black line), and Romania: Bucharest (green olive line), Iasi (blue line), Timisoara (brown line), on 24 September 2012. b. Daily mean aerosol size distribution derived from sun photometer measurements: over Greece: Xanthi (black line), and Romania: Bucharest (green olive line), Iasi (blue line), Timisoara (brown line), on 24 September 2012. (For interpretation of the references to color in this figure legend, the reader is referred to the web version of this article.)

following different trajectory paths. Concerning the air masses arriving at 3 km height over Greece and Romania, the situation is different as they generally originated from the Atlantic Ocean; a fact valid more for the Romanian site of Bucharest. Although they are passing close to the African continent (thus enriched in dust particles), the altitude of the air masses is quite elevated, and so these air masses were to be much poorer in dust particles. In this case, these air masses would consist of a mixture of dust with maritime aerosols. This is consistent with the low S values measured over Bucharest and Greece (36 and 45 sr), which agree with those recently reported by Mona et al. (2012).

The sun photometer data obtained within AERONET on 23 and 24 September are summarized in Table 3, for Xanthi, Timisoara, Bucharest and Iasi. We note that the daily mean AE values decrease when mixed dust particles arrive above the corresponding stations. This is due to the fact that mineral dust contains rather large (small AE values) particles. In terms of the AOD, which is an extensive parameter and depends on the particles' concentration, dust particles will be added to the existing mixed continental polluted/smoke aerosols. As consequence, the AOD increases. Thus, the mixing of Saharan dust with continental polluted/smoke aerosols results in a modification of both intensive (AE) and extensive (AOD) optical properties, therefore, the column aerosol microphysical properties.

The AERONET sun photometer retrievals for 24 September show that the fine mode fraction decreased over Romania starting in the morning (Fig. 9a). The first station where coarse dust particles arrived is Timisoara (around 08:00 UTC), followed soon by Bucharest (around 08:30 UTC) and later by Iasi (around 11:00 UTC). This corresponds to the time when the three lidars detected the dust layer in the free troposphere (Fig. 3). While in Timisoara and Bucharest coarse particles were predominant for the entire day, Iasi station was only for several hours (up to 13:30 UTC) under the influence of mineral dust. In Greece, the fine mode fraction remains constantly low (<0.5) starting from 23 September. Typical dust size distributions are observed (Fig. 9b) at all stations (Dubovik et al., 2002), with a high peak of coarse mode. Similar size distributions were depicted for Bucharest, Timisoara and Xanthi (Athens and Oxylythos) stations, while for Iasi tend to have more an urban behavior (smaller particles).

To corroborate the mixing of the aerosol particles sampled during AGRO over Greece and Romania we run the FLEXPART model for the measured aerosol layers over all measurement sites. When running in backward mode, FLEXPART can be used to estimate the sensitivity of measured concentrations to potential sources at different regions. This sensitivity is calculated as the residence time of simulated back-trajectories over a specific source region; high sensitivity values (i.e. residence time) values indicate greater change that aerosols at a specific region are mixed in the air mass and transported to the measurement site. Thus, in Fig. 10 we present the sensitivity to the total column (left) and to ground sources (right) for two selected cases. Fig. 10a shows the retro-plume for the aerosol layer sampled over Athens (16:45–17:15 UTC) on 24 September at 3.5 to 4 km height. The ground

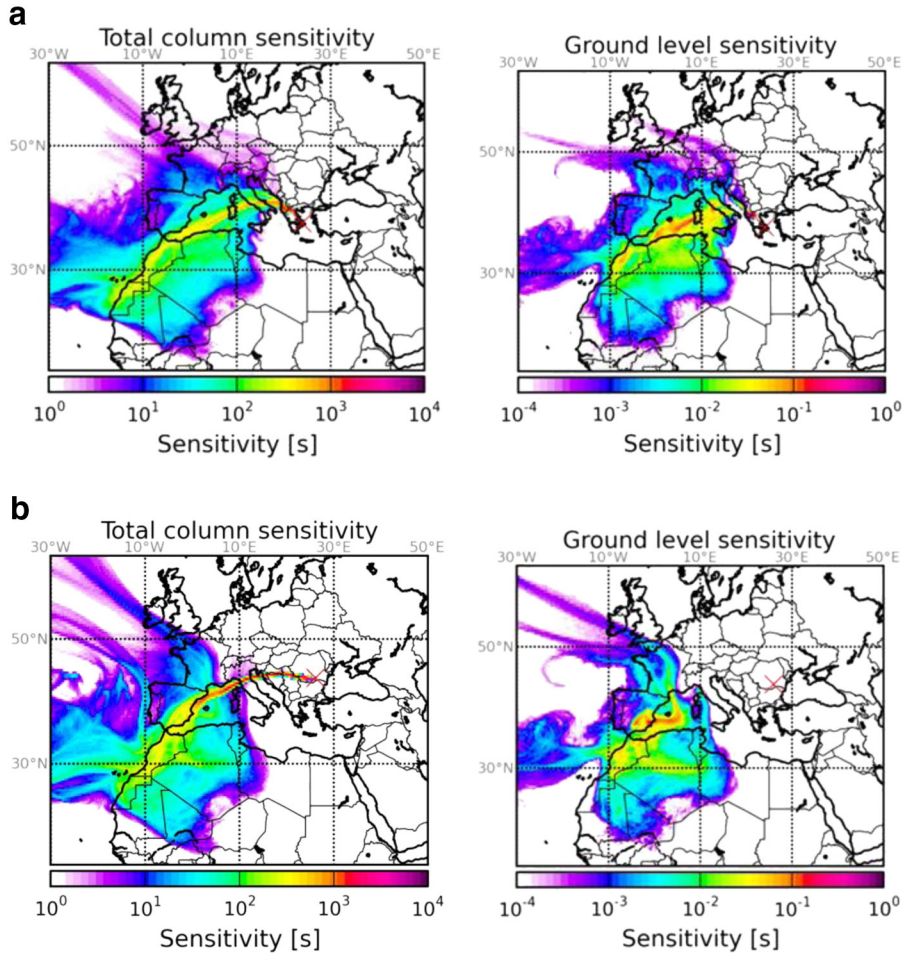


**Fig. 10.** a. FLEXPART retro-plume for Athens. Total column sensitivity (left) and ground level sensitivity (right) for aerosol at 3500–4000 m (16:45–17:15 UTC) on 24 September 2012. The red cross indicates the end point of the retro-plume. b. FLEXPART retro-plume for Bucharest. Total column sensitivity (left) and ground level sensitivity (right) for aerosol at 2000–2500 m (10:00–10:30 UTC) on 24 September 2012. The red cross indicates the end point of the retro-plume. (For interpretation of the references to color in this figure legend, the reader is referred to the web version of this article.)

level sensitivity plot indicates possible dust source location in northern Morocco and northern Algeria; moreover, these regions are also the source of biomass burning particles (cf Fig. 5), as it was previously mentioned. Fig. 10b shows the retro-plume for the second aerosol layer sampled over Bucharest (10:00–10:30 UTC) on 24 September at 2 to 2.5 km height. The ground level sensitivity plot indicates similar overall sources, but the relative strength is different: there is much stronger influence from Morocco desert and less from northern Algeria, as in the case of Athens; thus we expect the influence of forest biomass burning particles to be less strong, and a certain content of maritime aerosols from northern Atlantic to be present. The total column sensitivity indicates the relative direct transport of aerosols overpassing northern Italy before arriving over Bucharest. This is in agreement with the measured linear depolarization ratio of the order of 25% (cf. Fig. 6b), which is of the same order as the one observed in similar cases of mixture of dust and biomass burning aerosols (Tesche et al., 2009; Müller et al., 2013).

We also run the DREAM model to simulate dust concentration cross sections along Athens–Oxylithos–Xanthi–Bucharest (Fig. 11a and b). Thus, in Fig. 11a we present the vertical cross sections of the aerosol dust concentration (in  $\mu\text{g}/\text{m}^3$ ) and wind barbs (in m/s) along Athens–Oxylithos–Xanthi–Bucharest, for 09:00 UTC and 12:00 UTC on 24 September 2012 (upper and lower panel, respectively); while in Fig. 11b, we present similar cross sections for 15:00 UTC and 18:00 UTC, for the same date as previously. From this figure we see that dust, over all experimental sites, is confined below 3.5–4 km, as depicted by our lidar measurements (Fig. 3). Similarly, in Fig. 11c we

present the simulated by DREAM horizontal cross section of the aerosol dust concentration (in  $\mu\text{g}/\text{m}^3$ ) along the Athens–Oxylithos–Xanthi–Bucharest on 24 September 2012, at 1.4 km height (18:00 UTC), where we can see that Oxylithos shows similar dust concentrations as Bucharest (of the order of 20–50  $\mu\text{g}/\text{m}^3$ ); it is worthy to note that these values are quite similar to those to be presented later in this paper, as retrieved by POLIPHON, regarding the non-spherical data at Oxylithos site, but quite lower than those at Bucharest site.

Furthermore, a quantitative analysis of the aerosol load was performed for the Bucharest and Oxylithos stations, where depolarization measurements were available. Since Oxylithos's lidar does not have multi-wavelength capabilities, we used the POLIPHON code for the comparison. The retrieval variability was tested on Bucharest lidar data, for which both LIRIC and POLIPHON computations were made. Note that, although both codes use as inputs depolarization lidar and sun photometer data, each method is different and provides different outputs. POLIPHON uses the linear particle depolarization ratio to separate spherical and non-spherical particle's contribution to optical profiles. Volume concentration of each is obtained by using a size-dependent intensive parameter retrieved from sun photometer measurements, which represents a mean over the entire atmospheric column. Volume concentration profiles of spherical and non-spherical particles are therefore obtained from POLIPHON. LIRIC uses multi-wavelength lidar signals to calculate extensive optical parameters (backscatter coefficients), as well as column integrated volume concentration (also extensive) to finally provide volume concentration profiles

for fine (diameter  $< 1 \mu\text{m}$ ), coarse spherical and coarse spheroids particles (diameter  $> 1 \mu\text{m}$ ).

In Fig. 12a we present the comparison of aerosol mass concentration retrieved by LIRIC and POLIPHON for the Bucharest station for 24 September 2012. Aerosol backscatter and depolarization profiles at 11:00, 16:00, and 19:00 UTC were used as input data for these two codes. Based on the principle described in Section 2, LIRIC provides the coarse spherical, coarse spheroids and fine mode's volume concentration profiles, while POLIPHON provides the high and low depolarizing aerosol volume concentration profiles. We considered that the mineral dust particles are represented by the coarse spheroids from LIRIC and by the high depolarizing component from POLIPHON. The fine particles and the coarse spherical particles from LIRIC were added and compared to the low depolarizing particles from POLIPHON.

For POLIPHON algorithm, the fine and coarse aerosol backscatter coefficient was calculated assuming a linear particle depolarisation ratio of 0.35 for coarse particles and 0.02 for fine ones. The lidar ratio of dust was assumed 55 sr (e.g. Ansmann et al., 2012). In order to convert the volume concentration from the two algorithms to mass concentration, we used a typical density for dust (coarse spheroids) of  $2.6 \text{ g/cm}^3$  (Hess et al., 1998), a value which is consistent with a mixture of typical mineral components (Lide, 2004) and a typical density for fine aerosol of  $1.6 \text{ g/cm}^3$  for the European continent (Putaud et al., 2004; Cozic et al., 2008). LIRIC profiles (dark colors in Fig. 12a) show high concentrations of non-spherical particles (up to  $120 \mu\text{g/m}^3$ ) between 1.8 and 3.1 km height (11:00 UTC) and up to  $75 \mu\text{g/m}^3$  between 1.3 and 2.8 km altitude in the afternoon at 16:00 UTC. Lower loads are visible at 11:00 UTC between 1.3 and 1.8 km altitude, as well as above 3.0 km

at 16:00 UTC. In the evening, a homogeneous load (up to  $60 \mu\text{g/m}^3$ ) of non-spherical particles is visible from 1.0 to 3.0 km altitude. Spherical particles are present in low concentrations (up to  $30 \mu\text{g/m}^3$ ) between 1.3 and 3.8 km the entire day.

The POLIPHON assumption that fine and coarse aerosol modes correspond to spherical and non-spherical particles was checked by comparing the estimated backscatter coefficient profiles for each mode with the retrieved aerosol optical depth of the AERONET photometer. Specifically, following Ansmann et al. (2012), we computed the column-integrated backscatter coefficient for each mode ( $\text{CBf}$ ,  $\text{Cbc}$ ) and compared these values with AERONET's fine and coarse mode AOD values. For example, in the case of 24th September (11:00 UTC), the ratios  $\text{AODc/Cbc}$  and  $\text{AODf/Cbf}$ , which can be considered as "columnar lidar ratio", were calculated to be 59 and 47 sr, respectively, in good agreement with expected values of Saharan dust and aged smoke lidar ratio (e.g. Müller et al., 2007; Nicolae et al., 2013). This is a strong indication that our assumption that the coarse mode corresponds to non-spherical particles is valid.

LIRIC does not provide any indication on the uncertainty of the retrievals. On the other hand, the assumptions made when using POLIPHON to convert single wavelength optical data to mass concentration lead to errors that are difficult to estimate (e.g. are the properties of "pure" components: depolarization ratio, lidar ratio, mass density, well known?). POLIPHON profiles for Bucharest station (Fig. 12b, red and blue curves) were obtained by using fixed values for the specific particle depolarization ratios of the spherical (2%) and non-spherical particles (35%), and variable conversion factors (volume concentration / extinction) from 0.62 to 0.97  $\mu\text{m}$ . The lower value of the conversion factor

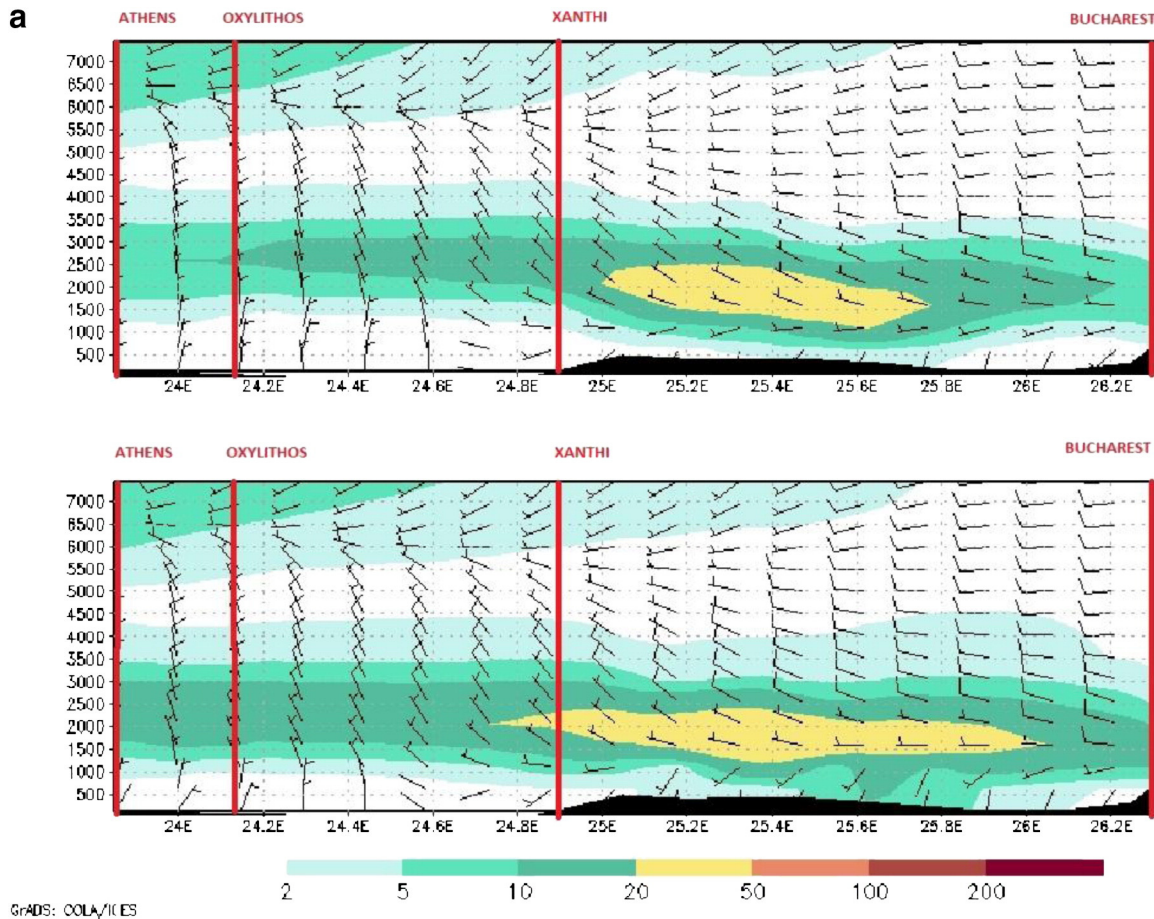


**Fig. 11.** a. Vertical cross sections of the aerosol dust concentration (in  $\mu\text{g/m}^3$ ) and wind barbs (in m/s) along Athens–Oxylithos–Xanthi–Bucharest, for 09:00 UTC and 12:00 UTC on 24 September 2012 (upper and lower panel, respectively). b. Vertical cross sections (simulated by DREAM) of the aerosol dust concentration (in  $\mu\text{g/m}^3$ ) and wind barbs (in m/s) along Athens–Oxylithos–Xanthi–Bucharest, for 15:00 UTC and 18:00 UTC on 24 September 2012 (upper and lower panel, respectively). c. Horizontal cross section (simulated by DREAM) of the aerosol dust concentration (in  $\mu\text{g/m}^3$ ) along Athens–Oxylithos–Xanthi–Bucharest on 24 September 2012, at 1360 m height (18:00 UTC).

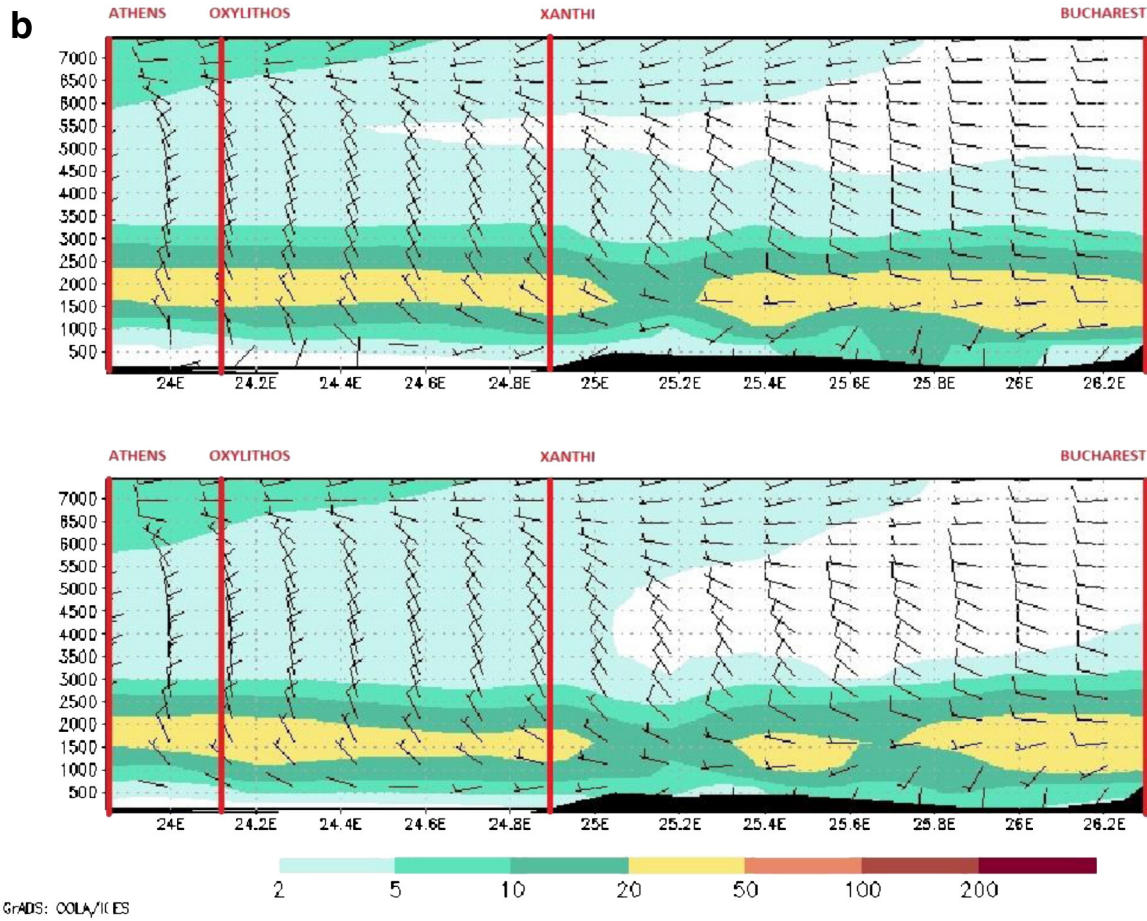


Fig. 11 (continued).

was obtained by OPAC simulation for mineral dust (Hess et al., 1998). AERONET retrieval was used as the higher value.

A detailed discussion of the error in each steps of the algorithm is given in Tesche et al. (2009), Ansmann et al. (2011), and Ansmann et al. (2012) where the total mass profile uncertainty is estimated to be 30–60%. A sensitivity analysis performed in selected cases of our study, using the range of these parameters found in literature, corroborates these findings; the uncertainty in the aerosol extinction profiles is below 25% for all altitudes with significant aerosol layers.

In our case only the statistical error and the uncertainty of the conversion factor were considered when computing the overall error of the POLIPHON mass concentration. Because no in situ data at the altitudes of the layers were collected, we performed a cross-validation of the LIRIC and POLIPHON retrievals. We computed the relative difference between the mass concentration obtained with LIRIC and POLIPHON respectively, separately for spherical (blue and light blue curves) and non-spherical particles (red and light red curves), as in Eq. (1):

$$\Delta_{\text{spherical}} = \frac{(m_{\text{spherical}}^{\text{POLIPHON}} - m_{\text{spherical}}^{\text{LIRIC}})}{m_{\text{spherical}}^{\text{LIRIC}}}, \Delta_{\text{non-spherical}} = \frac{(m_{\text{non-spherical}}^{\text{POLIPHON}} - m_{\text{non-spherical}}^{\text{LIRIC}})}{m_{\text{non-spherical}}^{\text{LIRIC}}} \quad (1)$$

We see in Fig. 12a that  $\Delta_{\text{non-spherical}}$  is smaller than  $\pm 20\%$  with significant aerosol loads (e.g. AOD > 0.15 at 532 nm, within the layer 1.8–3.1 km (11:00 UTC) and the layer 1.3–2.8 km (16:00 UTC)). Negative

values obtained generally for  $\Delta_{\text{spherical}}$  within the layers (between 1.3 and 3.8 km altitude at 11:00 UTC, and between 1.5 and 3.8 km altitude at 16:00 UTC) show that POLIPHON underestimates the mass concentration of spherical particles. This is probably due to the underestimation of the corresponding conversion factor which does not include the contribution of coarse spherical particles. For Bucharest station, where spherical particles are mostly confined in the fine mode, the relative difference within well-defined layers goes down to  $-50\%$ . The disagreement is expected to be larger for Greek stations, where maritime aerosols (large spherical particles) are generally present. For regions with low aerosol loads (e.g. with AOD < 0.01 at 532 nm, for heights below 1.5 and above 3.8 km) the uncertainty of both LIRIC (not shown) and POLIPHON is much higher, and consequently is their relative difference. We also note some differences in terms of layer bottoms and tops, both for spherical and non-spherical particles. In the middle of the layers,  $\Delta_{\text{spherical}}$  and  $\Delta_{\text{non-spherical}}$  are almost constant; this means that the vertical variation of the mass concentration is well captured by both codes. Close to the edges, the absolute value of  $\Delta_{\text{spherical}}$  and  $\Delta_{\text{non-spherical}}$  increases rapidly. This is due to the different effective spatial resolutions and smoothing parameters used by the two codes.

A special feature is represented by the two distinct layers around 11:00 UTC. For these layers POLIPHON and LIRIC return a mixing of spherical and non-spherical particles, but with different mixing ratios. Non-spherical particles are predominant in the upper layer, and a considerable contribution of spherical particles is present in the lower layer. Conform to the HYSPLIT trajectories (Fig. 4b), the 2 layers detected in this time interval have different origins: the source of the aerosol layer around 2 km is located in N. Africa (Algeria), while the source of the upper aerosol layer (around 3 km) is located in NW Africa

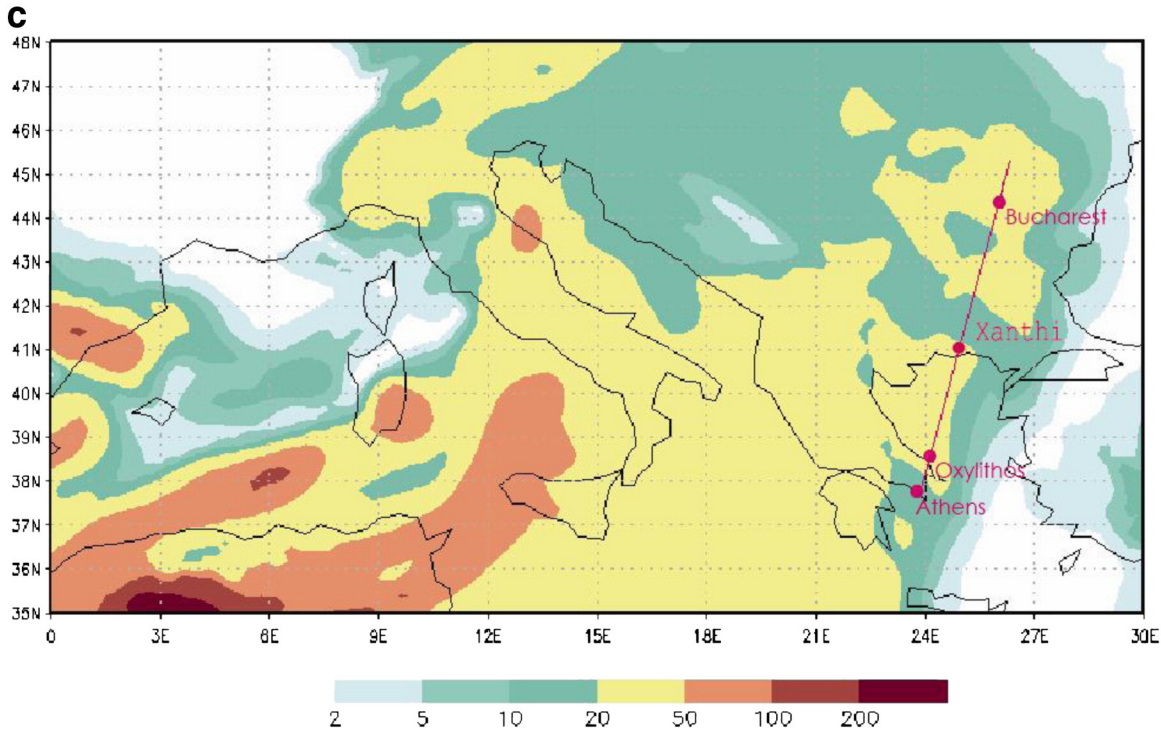


Fig. 11 (continued).

(Morocco). Different aerosol origins and paths may reflect in different aerosol compositions, which is the case here. The air masses arriving at 2 km above Bucharest, have traveled at low altitudes over Algeria ( $<0.5$  km) where dense fires were detected by MODIS in this period, as previously discussed. As a consequence, smoke particles were mixed and transported together with the mineral dust ones. On the other hand, the air masses arriving at 3 km above Bucharest have traveled at altitudes around 2–3 km along the west coast of Africa and south Spain, where MODIS/Firemap shows only few fire spots (cf. Figs. 3b and 5). A predominance of mineral dust mixed with maritime aerosols is also evidenced by FLEXPART ground level sensitivity plot for this layer (Fig. 10b). For the next time interval (16:00 UTC), the fine particles seem to be lifted to higher altitudes and mixed with the non-spherical up to 2.8 km height and a then a new distinct layer appears above 3 km height, having a lower particle load. In conclusion, a reasonable agreement was found between LIRIC and POLIPHON, especially for the retrievals of the non-spherical particles' mass concentrations within layers with significant aerosol load.

Additionally, we used POLIPHON to retrieve the mineral dust mass concentration profiles over Oxylithos, with similar assumptions as for Bucharest, and made a direct comparison of the mineral dust loads in Romania (Bucharest) and Greece (Oxylithos). As previously mentioned no simultaneous photometer measurements were available at the second site; thus, we estimated the coarse mode volume-to-extinction ratio by examining photometer measurements performed at Xanthi station, which was on the same air mass trajectory as Oxylithos conform to FLEXPART simulations. Although located at a long distance from Athens and Oxylithos (~350 km), the Xanthi station sampled similar air masses as those over Oxylithos, in terms of the atmospheric column, without being influenced by the urban pollution.

In the case of Oxylithos only the dust concentration is retrieved reliably. The aerosol measured at lower altitudes can be affected by marine aerosol, which the POLIPHON algorithm would wrongly classify as fine-mode. In addition the volume-to-extinction ratio for measured by AERONET for the fine mode could not be applied of Oxylithos case as this mode is mostly affected by local sources. The coarse mode's mass

retrieval however is not affected by these issues and can be reliably retrieved. The effect of topography on the coarse mode should be small, as the main dust load is located in the free troposphere.

On 24 September Xanthi measured very steady aerosol volume-to-AOD values of  $0.85 \mu\text{m}$ ; thus, we assume that this value can be used for the Oxylithos measurements. Additionally, for 19:00 UTC we also derived an estimate of the fine mode aerosol mass profile, using an extinction coefficient profile obtained by the Raman lidar over Athens. As described previously the dust concentration values over Oxylithos are affected by important uncertainties and thus are provided here only for qualitative purposes.

Thus, in Fig. 12b we present the dust mass concentration vertical profiles for the Oxylithos (black and cyan lines) and Bucharest (red and blue lines) stations obtained with POLIPHON. These profiles are given for 11:00, 12:00, 16:00 and 19:00 UTC of 24 September. The overall dust mass concentration was higher in Bucharest than Oxylithos, but the layer altitudes, as well as their shape, remain quite similar. The main difference, however, is the low altitude mixed layer (dust and smoke) arriving over Bucharest before noon, originating from N. Africa, which is not visible in the Oxylithos aerosol vertical profiles.

Furthermore, for Oxylithos, at 11:00 and 12:00 UTC, we observe one single aerosol layer between 2.3 and 3.5 km and 1.7 and 2.7 km heights, respectively, peaking around  $60 \mu\text{g}/\text{m}^3$ . Later, at 16:00 UTC, the previous aerosol layer has been gradually mixed with cleaner air masses having lower dust loads, while two new dust layers are formed later: the first between 0.8 and 2.1 km and the second, between 3 and 4.5 km height, both peaking around  $72 \mu\text{g}/\text{m}^3$ . Finally, at 19:00 UTC the aerosol load has been diminished compared to the one at 16:00 UTC, being confined between 1 and 4 km, with mass concentrations mostly below  $50 \mu\text{g}/\text{m}^3$ , which are superposed by a stronger one from 3 to 4 km height, peaking around  $52 \mu\text{g}/\text{m}^3$ . From the fine (spherical) aerosol mode profile available at 19:00 UTC, we can see the presence of small particles up to 4.5 km height, the lower ones (below 2.5 km) are due to local anthropogenic particles, while the higher ones (between 3 and 4 km) originated probably from distant sources (forest fires in N. Africa), as simulated by FLEXPART and measured by MODIS sensor, as previously discussed. The difference on the aerosol mass concentrations observed is mostly

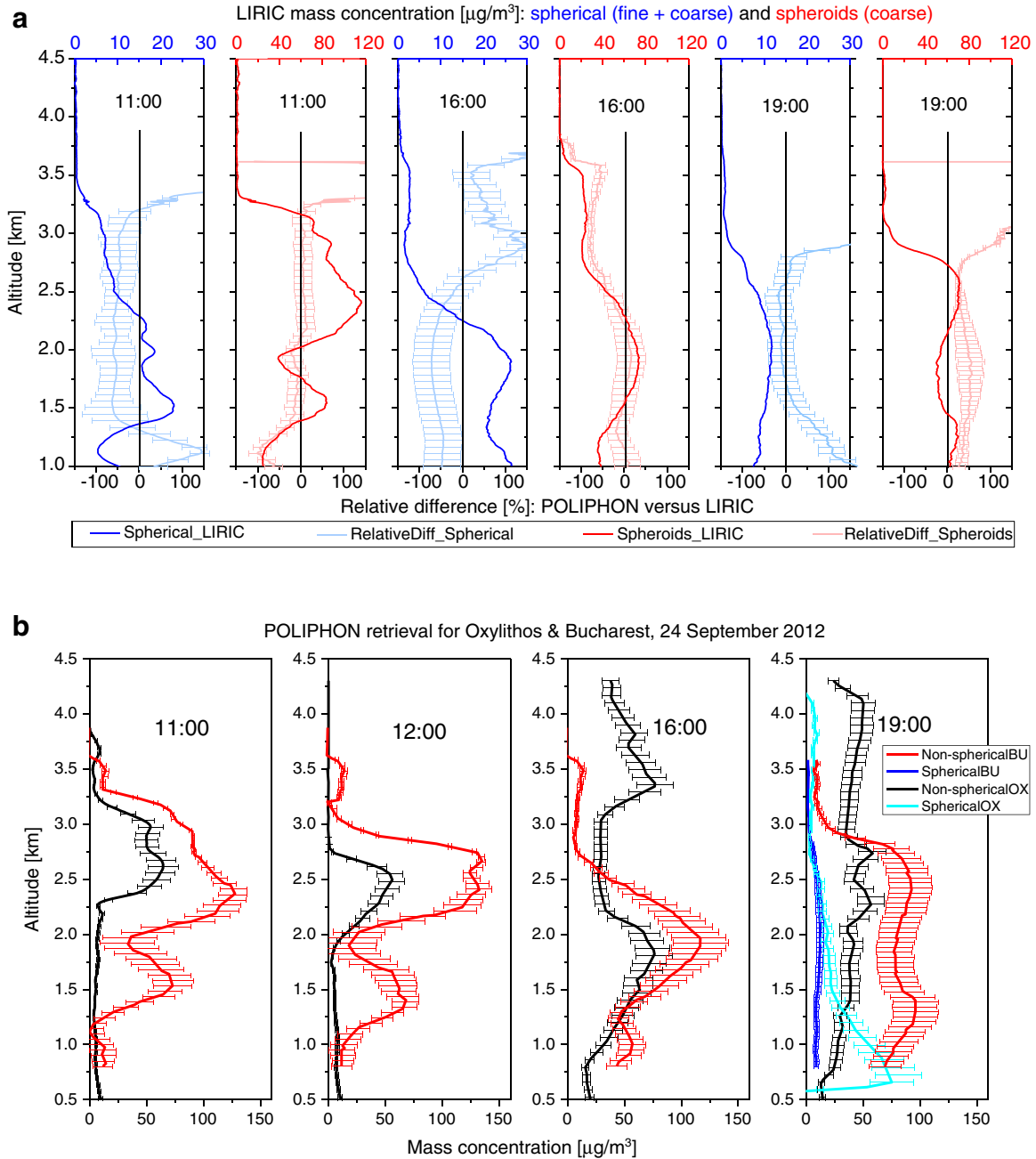


**Fig. 12.** a. POLIPHON to LIRIC relative difference of the spherical and non-spherical particles' mass concentration (in  $\mu\text{g}/\text{m}^3$ ) on 24 September 2012 for Bucharest at 11:00 and 16:00 UTC. b. Comparison between POLIPHON retrieved mass concentration of non-spherical particles detected at Oxylibithos (black lines) and Bucharest (red lines) on 24 September 2012 at 11:00 UTC, 12:00 UTC, 16:00 UTC and 19:00 UTC. Cyan and blue curves represent the mass concentration of spherical particles as retrieved by POLIPHON at 19:00 UTC for Oxylibithos and Bucharest, respectively. (For interpretation of the references to color in this figure legend, the reader is referred to the web version of this article.)

linked with the history of the air masses sampled over Bucharest and Oxylibithos; the mixing of non-spherical (dust) particles with continental polluted ones and/or biomass burning ones, during longer and different transport paths to Oxylibithos and Bucharest. During this event Bucharest is definitely more affected than Oxylibithos in non-spherical aerosol particles (higher concentrations) below 3 km height, which can be explained by the direct transport of higher dust loads over Bucharest than over Oxylibithos, due to different air mass trajectories.

## 5. Conclusions

Vertical profiles of the aerosol optical, size and mass properties were studied during a 2-day case study in the frame of a coordinated

experimental campaign in September 2012 based on the synergy of lidar and sunphotometers over five different sites, in Greece and Romania. Dust particles mixed with biomass burning and continental polluted ones were confined from the PBL region up to around 4–4.5 km height. High aerosol linear depolarization and lidar ratio values were measured inside the aerosol layers, ranging from 13 to 29% and 44 to 65 sr, respectively. AERONET retrievals showed that the fine mode fraction decreased over Romania starting in the morning of 24 September, when the dust event approached. The AOD values ranged from 0.13 to 0.26 at 532 nm, with a clear gradient from South to North, even when the Saharan dust outbreak was over all observing stations.

Moreover, LIRIC and POLIPHON codes were used/compared regarding the retrieved (fine/coarse, spherical/spheroid) aerosol mass

concentrations. LIRIC retrievals over Bucharest showed generally high mass concentrations of non-spherical particles (up to 120 µg/m<sup>3</sup>), while spherical particles were retrieved to be up to 30 µg/m<sup>3</sup>. When comparing the aerosol mass concentrations from LIRIC and POLIPHON retrievals over Bucharest, we found that their difference is smaller than ±20% for layers with significant non-spherical aerosol loads. On the other hand, when spherical particles are sampled, POLIPHON generally underestimates the aerosol mass concentrations. In the case of non-spherical particles, POLIPHON retrievals over Oxylythos and Bucharest showed similar in shape and extended dust layers up to 4–4.5 km heights, always the Bucharest mass concentration profiles (100–140 µg/m<sup>3</sup>) being higher (by a factor of 1.5–2) than the Oxylythos' ones (50–75 µg/m<sup>3</sup>). This is probably due to the fact that the lower altitude heights (below 2 km) at Oxylythos were mostly influenced by local clean air masses, while over Bucharest, these low altitude layers were influenced directly by fast moving air masses originating from N. Africa. In all cases, both sites were highly influenced by the dust particles, with higher values of the aerosol linear depolarization ratio over Oxylythos on 24 September (18–30%) than over Bucharest (12–23%). This difference has been related to mixing of non-spherical (dust) particles with continental polluted ones and/or biomass burning ones, during longer and different transport paths to Oxylythos and Bucharest.

While studying aerosol modification along Greece–Romania we showed that particles are always subject to mixing processes along their trajectories starting from their source regions to the sampling sites. This also is reflected into the values of their optical, microphysical and mass properties, showing that the particles may retain their non sphericity as they move from the desert regions to the continentally polluted ones, depending on the mixing processes taking part along their trajectories from their desert source region to our sampling sites.

## Acknowledgements

This work was supported by grants of the Romanian National Authority for Scientific Research project no. PN 09-27 01 03, 62EU/2009 and PN-II-RU-PD-2011-3-0082 and by the European Community's FP7-INFRASTRUCTURES-2010-1 under grant no. 262254-ACTRIS and by FP7-AAT-2008-RTD-1 under grant no. 233801. The research of AP and GT has been co-financed by the European Union (European Regional Development Fund—ERDF) and the General Secretariat for Research and Technology (GSRT) of the Greek Ministry of Education and Religious Affairs, in the framework of the National Strategic Reference Framework (NRSF)-2007–2013 (Bilateral Greek–Romanian R&T Cooperation 2011–2012) under grant no. ROM 36\_5\_ET30. This project has received funding from the European Union's Seventh Framework Program for research, development, and demonstration under grant agreement no. 289923–ITaRS. The air mass backward trajectories were computed with the Hybrid Single-Particle Lagrangian Integrated Trajectory (HYSPLIT-4.6) model developed at NOAA, USA. The FLEXPART model has been provided from <http://transport.nilu.no/flexpart>, while the meteorological maps were provided by the UK MetOffice (UKMO). AERONET data were provided by NASA/GSFC. We acknowledge the use of FIRMS data and imagery from the Land Atmosphere Near-real time Capability for EOS (LANCE) system operated by the NASA/GSFC/Earth Science Data and Information System (ESDIS) with funding provided by NASA/HQ. The Principal Investigators of the Bucharest, Iasi, Timisoara and Xanthi AERONET stations are gratefully acknowledged. Authors thank Slobodan Nickovic (Institute of Physics, University of Belgrade) for useful discussions and Slavko Petkovic (Republic Hydro-meteorological Service of Serbia) for assistance in performing the experiments and for preparing figures. Authors are also grateful to Republic Hydro-meteorological Service of Serbia for providing computing resources for model simulations. This research was partly funded by the project III43007 financed by the Ministry of Education and Science of the Republic of Serbia within the framework of integrated and interdisciplinary research for the period 2011–2014. The Biomedical

Research Foundation of the Academy of Athens (BRFAA) is acknowledged for the provision of the lidar mobile platform.

## References

- Abbatt JPD, Benz S, Cziczo DJ, Kanji Z, Lohmann U, Möhler O. Solid ammonium sulfate aerosols as ice nuclei: a pathway for cirrus cloud formation. *Science* 2006;313: 1770–3.
- Ackermann FA, Chung H. Radiative effects of airborne dust and regional energy budget at the top of the atmosphere. *J Appl Meteorol* 1992;31:223–36.
- Amiridis V, Wandinger U, Marinou E, Giannakaki E, Tsekeli A, Basart S, et al. Optimizing Saharan dust CALIPSO retrievals. *Atmos Chem Phys* 2013;13:12089–106. <http://dx.doi.org/10.5194/acp-13-12089-2013>.
- Andreae M, Crutzen P. Atmospheric aerosols: biochemical sources and role in atmospheric chemistry. *Science* 1997;276:1052–7.
- Angelini F, Gobbi GP. Some remarks about lidar data preprocessing and different implementations of the gradient method for determining the aerosol layers. *Ann Geophys* 2014;57:A0218. <http://dx.doi.org/10.4401/ag-6408>.
- Ansmann A, Riebesell M, Wandinger U, Weitkamp C, Voss E, Lahmann W, et al. Combined Raman elastic-backscatter lidar for vertical profiling of moisture, aerosol extinction, backscatter, and lidar ratio. *Appl Phys* 1992;B55:18–28.
- Ansmann A, Tesche M, Seifert P, Groß S, Freudenthaler V, Apituley A, et al. Ash and fine-mode particle mass profiles from EARLINET–AERONET observations over central Europe after the eruptions of the Eyjafjallajökull volcano in 2010. *J Geophys Res* 2011;116:D00U02. <http://dx.doi.org/10.1029/2010JD015567>.
- Ansmann A, Seifert P, Tesche M, Wandinger U. Profiling of fine and coarse particle mass: case studies of Saharan dust and Eyjafjallajökull/Grímsvötn volcanic plumes. *Atmos Chem Phys* 2012;12:9399–415. <http://dx.doi.org/10.5194/acp-12-9399-2012>.
- Balin I. Measurement and analysis of aerosols, cirrus-contrails, water vapor and temperature in the upper troposphere with the Jungfraujoch LIDAR system. EPFL Ph.D. Thesis, <http://infoscience.epfl.ch/record/33448>, 2004.
- Böckmann C, Wandinger U, Ansmann A, Bösenberg J, Amiridis V, Boselli A, et al. Aerosol lidar intercomparison in the framework of the EARLINET project: Part II—aeosol backscatter algorithms. *Appl Opt* 2004;43:977–89.
- Bösenberg J, Matthias V, Amodeo A, Amoirdis V, Ansmann A, Baldasano JM, et al. EARLINET: A European Aerosol Research Lidar Network. MPI-Report, 348. Hamburg, Germany: Max-Planck-Institut für Meteorologie; 2003. p. 1–191.
- Cerully KM, Raatikainen T, Lance S, Tkacik D, Tuitt P, Petäjä T, et al. Aerosol hygroscopicity and CCN activation kinetics in a boreal forest environment during the 2007 EUCAARI campaign. *Atmos Chem Phys* 2011;11:12369–86.
- Chaikovsky A, Dubovik O, Goloub P, Tanré D, Pappalardo G, Wandinger U, et al. Algorithm and software for the retrieval of vertical aerosol properties using combined lidar/radiometer data: Dissemination in EARLINET. In: Papayannis A, Balis D, Amiridis V, editors. Reviewed and revised papers presented at the 26th International Laser Radar Conference, Porto Heli, Greece; 2012. p. 399–402.
- Comerón A, Sicard M, Rocadenbosch F. Wavelet correlation transform method and gradient method to determine aerosol layering from lidar returns: some comments. *J Atmos Oceanic Tech* 2013;30:1189–93. <http://dx.doi.org/10.1175/JTECH-D-12-0023.1>.
- Cozic J, Verheggen B, Weingartner E, Crosier J, Bower KN, Flynn M, et al. Chemical composition of free tropospheric aerosol for PM1 and coarse mode at the high alpine site Jungfraujoch. *Atmos Chem Phys* 2008;8:407–23. <http://dx.doi.org/10.5194/acp-8-407-2008>.
- Di Giuseppe F, Riccio A, Caporaso L, Bonafè G, Gobbi GP, Angelini F. Automatic detection of atmospheric boundary layer height using ceilometer backscatter data assisted by a boundary layer model. *Q J R Meteorol Soc* 2011;138:649–63. <http://dx.doi.org/10.1002/qj.964>.
- Draxler RR, Stunder B, Rolph G, Talyor AD. *Hysplit 4 User's Guide*. Silver Spring, MD, USA: NOAA Air Resources Laboratory; 2009.
- Dubovik O, Holben B, Eck TF, Smirnov A, Kaufman YJ, King MD, Tanré D, Slutsker I. Variability of absorption and optical properties of key aerosol types observed in worldwide locations. *J. Atmos Sci* 2002;59:590–608. [http://dx.doi.org/10.1175/1520-0469\(2002\)059-0590:VOAAOP>2.0.CO;2](http://dx.doi.org/10.1175/1520-0469(2002)059-0590:VOAAOP>2.0.CO;2).
- Dubovik O, Smirnov A, Holben BN, King MD, Kaufman YJ, Eck TF, et al. Accuracy assessment of aerosol optical properties retrieved from AERONET sun and sky radiance measurements. *J Geophys Res* 2000;105:9791–806.
- Endlich RM, Ludwig F, Utte EE. An automated method for determining the mixing layer depth from lidar observations. *Atmos Environ* 1979;13:1051–6.
- Forster P, Ramaswamy V, Artaxo P, Bernstein T, Betts R, Fahey DW, et al. Changes in atmospheric constituents and in radiative forcing. In: Solomon S, Qin D, Manning M, Chen Z, Marquis M, Averyt KB, Tignor M, Miller HL, editors. *Climate Change 2007: The Physical Science Basis. Contribution of Working Group I to the Fourth Assessment Report of the Intergovernmental Panel on Climate Change*. Cambridge, UK: Cambridge University Press; 2007. p. 129–234.
- Freudenthaler V, Esselborn M, Wiegner M, Heese B, Tesche M, Ansmann A, et al. Depolarization ratio profiling at several wavelengths in pure Saharan dust during SAMUM 2006. *Tellus* 2009;61B:165–79.
- Giannakaki E, Balis DS, Amiridis V, Zerefos CS. Optical properties of different aerosol types: seven years of combined Raman–elastic backscatter lidar measurements in Thessaloniki, Greece. *Atmos Meas Tech* 2010;3:569–78.
- Giglio L, Descloitres J, Justice CO, Kaufmann Y. An enhanced contextual fire detection algorithm for MODIS. *Remote Sens Environ* 2003;87:273–82.
- Guerrero-Rascado JL, Olmo FJ, Avilés-Rodríguez I, Navas-Guzm F, Pérez-Ramírez D, Lyamani H, et al. Extreme Saharan dust event over the southern Iberian Peninsula

- in September 2007: active and passive remote sensing from surface and satellite. *Atmos Chem Phys* 2009;9:8453–69.
- Heinold B, Tegen I, Bauer S, Wendisch M. Regional modelling of Saharan dust and biomass-burning smoke. *Tellus* 2011;B63:800–13. <http://dx.doi.org/10.1111/j.1600-0889.2011.00574.x>.
- Hess M, Koepke P, Schultz J. Optical properties of aerosols and clouds: the software package OPAC. *Bull Am Meteorol Soc* 1998;79:831–44.
- Holben BN, Eck TF, Slutsker I, Tanré D, Buis JP, Setzer A, et al. AERONET—a federated instrument network and data archive for aerosol characterization. *Remote Sens Environ* 1998;66:1–16. [http://dx.doi.org/10.1016/S0034-4257\(98\)00031-5](http://dx.doi.org/10.1016/S0034-4257(98)00031-5).
- Holben BN, Eck TF, Slutsker I, Smirnov A, Sinyuk A, Schafer J, et al. AERONET's version 2.0 quality assurance criteria. *Proc SPIE* 2006;6408:6408Q. <http://dx.doi.org/10.1117/12.706524>.
- Janjic ZI, Gerrity Jr JP, Nickovic S. An alternative approach to non hydrostatic modelling. *Mon Weather Rev* 2011;129:1164–78.
- Kanakidou M, Mihalopoulos N, Kindap T, Im U, Vrekoussis M, Gerasopoulos E, et al. Megacities as hot spots of air pollution in the East Mediterranean. *Atmos Environ* 2011;45:1223–35.
- Kanitz T, Ansmann A, Seifert P, Engelmann R, Kalisch J, Althausen D. Radiative effect of aerosols above the northern and southern Atlantic Ocean as determined from shipborne lidar observations. *J Geophys Res* 2013;118:12556–65. <http://dx.doi.org/10.1002/2013JD019750>.
- Klett J. Stable analytical inversion for processing lidar returns. *Appl Opt* 1981;20:211–20.
- Klett J. Lidar inversion with variable backscatter extinction ratios. *Appl Opt* 1985;24:1638–43.
- Kokkalis P, Papayannis A, Mamouri RE, Tsaknakis G, Amiridis V. The EOLE lidar system of the National Technical University of Athens. In: Papayannis A, Balis D, Amiridis V, editors. Reviewed and revised papers presented at the 26th International Laser Radar Conference, 25–29 June 2012, Porto Heli, Greece; 2012. p. 629–32.
- Kokkalis P, Papayannis A, Amiridis V, Mamouri RE, Veselovskii I, Kolgotin A, et al. Optical, microphysical, mass and geometrical properties of aged volcanic particles observed over Athens, Greece, during the Eyjafjallajökull eruption in April 2010 through synergy of Raman lidar and sunphotometer measurements. *Atmos Chem Phys* 2013;13:9303–20.
- Koulouri E, Saarikoski S, Theodosi C, Markaki Z, Gerasopoulos E, Kouvarakis G, et al. Chemical composition and sources of fine and coarse aerosol particles in the Eastern Mediterranean. *Atmos Environ* 2008;42:6542–50. <http://dx.doi.org/10.1016/j.atmosenv.2008.04.010>.
- Lance S, Nenes A, Mazzoleni C, Dubey MK, Gates H, Varutbangkul V, et al. Cloud condensation nuclei activity, closure, and droplet growth kinetics of Houston aerosol during the Gulf of Mexico Atmospheric Composition and Climate Study (GoMACCS). *J Geophys Res* 2009;114:D00F15. <http://dx.doi.org/10.1029/2008JD011699>.
- Landulfo E, Papayannis A, De Freitas AZ, Vieira Jr ND, Souza RF, Gonç A, et al. Tropospheric aerosol observations in São Paulo, Brazil using a compact lidar system. *Int J Remote Sens* 2005;26:2797–816.
- Lathem TL, Beyersdorf AJ, Thornhill KL, Winstead EL, Cubison MJ, Hecobian A, et al. Analysis of CCN activity of Arctic aerosol and Canadian biomass burning during summer 2008. *Atmos Chem Phys* 2013;13:2735–6.
- Lelieveld J, Berresheim H, Borrmann S, Crutzen PJ, Dentener FJ, Fischer H, et al. Global Air pollution crossroads over the Mediterranean. *Science* 2002;298:794–9.
- Lide D. CRC Handbook of Chemistry and Physics 2004–2005. A Ready-Reference Book of Chemical and Physical Data. USA: CRC Press; 2004.
- Mamouri RE, Amiridis V, Papayannis A, Giannakaki E, Tsaknakis G, Balis DS. Validation of CALIPSO space-borne-derived attenuated backscatter coefficient profiles using a ground-based lidar in Athens, Greece. *Atmos Meas Tech* 2009;2:513–22.
- Mamouri RE, Ansmann A, Nisantzi A, Kokkalis P, Schwarz A, Hadjimitsis D. Low Arabian dust extinction-to-backscatter ratio. *Geophys Res Lett* 2013;40:4762–6. <http://dx.doi.org/10.1002/grl.50898>.
- Matthias V, Freudenthaler V, Amodeo A, Balin I, Balis D, Bösenberg J, et al. Aerosol lidar inter-comparison in the framework of the EARLINET project. 1. Instruments. *Appl Opt* 2004;43:961–76.
- Mattis I, Ansmann A, Müller D, Wandinger U, Althausen D. Dual-wavelength Raman lidar observations of the extinction-to-backscatter ratio of Saharan dust. *Geophys Res Lett* 2002;29:1306. <http://dx.doi.org/10.1029/2002GL014721>.
- Meloni D, di Sarra A, Di Iorio T, Fiocco G. Influence of the vertical profile of Saharan dust on the visible direct radiative forcing. *J Quant Spectrosc Radiat Transf* 2005;93:397–413.
- Mona L, Amodeo A, Pandolfi M, Pappalardo G. Saharan dust intrusions in the Mediterranean area: three years of Raman lidar measurements. *J Geophys Res* 2006;111:D16203. <http://dx.doi.org/10.1029/2005JD006569>.
- Mona L, Liu Z, Müller D, Omar A, Papayannis A, Pappalardo G, et al. Lidar measurements for desert dust characterization: an overview. *Adv Meteorol* 2012;2012. <http://dx.doi.org/10.1155/2012/356265>.
- Moore RH, Karydis VA, Capps SL, Lathem TL, Nenes A. Droplet number uncertainties associated with CCN: an assessment using observations and a global model adjoint. *Atmos Chem Phys* 2013;13:4235–51.
- Müller D, Ansmann A, Mattis I, Tesche M, Wandinger U, Althausen D, et al. Aerosol-type-dependent lidar ratios observed with Raman lidar. *J Geophys Res* 2007;112:D16202. <http://dx.doi.org/10.1029/2006JD008292>.
- Müller D, Veselovskii I, Kolgotin A, Tesche M, Ansmann A, Dubovik O. Vertical profiles of pure dust and mixed smoke-dust plumes inferred from inversion of multi-wavelength Raman polarization lidar data and comparison to AERONET retrievals and in situ observations. *Appl Opt* 2013;52:3178–202.
- Müller D, Wandinger U, Ansmann A. Microphysical particle parameters from extinction and backscatter lidar data by inversion with regularization: theory. *Appl Opt* 1999;38:2346–57.
- Nemuc A, Vasilescu J, Talianu C, Belegante L, Nicolae D. Assessment of aerosol's mass concentrations from measured linear particle depolarization ratio (vertically resolved) and simulations. *Atmos Meas Tech* 2013;6:3243–55. <http://dx.doi.org/10.5194/amt-6-3243-2013>.
- Nickovic S. Distribution of dust mass over particle sizes: impacts on atmospheric optics. 4th ADEC Workshop—Aeolian Dust Experiment on Climate Impact, 26–28 January, Nagasaki, Japan; 2005. p. 357–60.
- Nickovic S, Kallos G, Papadopoulos A, Kakaliagou O. A model for prediction of desert dust cycle in the atmosphere. *J Geophys Res* 2001;106(D16):18113–29. <http://dx.doi.org/10.1029/2000JD900794>.
- Nicolae D, Talianu C, Mamouri RE, Carstea E, Papayannis A, Tsaknakis G. Air mass modification processes over the Balkans area detected by aerosol lidar techniques. *Optoelectron Adv Mater* 2008;2:394–402.
- Nicolae D, Nemuc A, Müller D, Talianu C, Vasilescu J, Belegante L, et al. Characterization of fresh and aged biomass burning events using multi-wavelength Raman lidar and mass spectrometry. *J Geophys Res* 2013;118:2956–65. <http://dx.doi.org/10.1002/jgrd.50324>.
- Noh YM, Müller D, Hanlim L, Lee KH, Kim K, Shin S, et al. Estimation of radiative forcing by the dust and non-dust content in mixed East Asian pollution plumes on the basis of depolarization ratios measured with lidar. *Atmos Environ* 2012;61:221–31.
- O'Neill NT, Eck TF, Smirnov A, Holben BN, Thulasiraman S. Spectral discrimination of coarse and fine mode optical depth. *J Geophys Res* 2003;108(D17):4559–73. <http://dx.doi.org/10.1029/2002JD002975>.
- Pandis S, Wexler S, Seinfeld J. Dynamics of tropospheric aerosol. *J Phys Chem* 1995;99:9646–59. <http://dx.doi.org/10.1021/j100024a003>.
- Papayannis A, Amiridis V, Mona L, Tsaknakis G, Balis D, Bösenberg J, et al. Systematic lidar observations of Saharan dust over Europe in the frame of EARLINET (2000–2002). *J Geophys Res* 2008;113:D10204. <http://dx.doi.org/10.1029/2007JD009028>.
- Papayannis A, Mamouri RE, Amiridis V, Remoundaki E, Tsaknakis G, Kokkalis P, et al. Optical-microphysical properties of Saharan dust aerosols and composition relationship using a multi-wavelength Raman lidar, in situ sensors and modelling: a case study analysis. *Atmos Chem Phys* 2012;12:4011–32.
- Papayannis A, Mamouri RE, Kokkalis P, Amiridis V, Kristiansen NI, Stohl A, et al. Optical properties and vertical extension of ash layers over the Eastern Mediterranean as observed by Raman lidars during the Eyjafjallajökull eruption (May 2010). *Atmos Environ* 2012b;48:56–65.
- Pappalardo G, Amodeo A, Pandolfi M, Wandinger U, Ansmann A, Bösenberg J, et al. Aerosol lidar intercomparison in the framework of EARLINET. Part III. Raman lidar algorithm for aerosol extinction, backscatter and lidar ratio. *Appl Opt* 2004;43:5370–585.
- Pappalardo G, Wandinger U, Mona L, Hebsch A, Mattis I, Amodeo A, et al. EARLINET correlative measurements for CALIPSO: first intercomparison results. *J Geophys Res* 2010;115:D00H19. <http://dx.doi.org/10.1029/2009JD012147>.
- Pejanovic G, Vukovic A, Vujadinovic M, Dacic M. Assimilation of satellite information on mineral dust using dynamic relaxation approach. *Geophys Res Abstr* 2010;12:EGU2010-7353.
- Pérez C, Sicard M, Jordà O, Comeron A, Baldasano JM. Summertime re-circulations of air pollutants over the North-Eastern Iberian coast observed from systematic EARLINET lidar measurements in Barcelona. *Atmos Environ* 2004;38:3983–4000.
- Prospero JM, Ginoux P, Torres O, Nicholson SE, Gill TE. Environmental characterization of global sources of atmospheric soil dust identified with the Nimbus 7 total ozone mapping spectrometer (TOMS) absorbing aerosol product. *Rev Geophys* 2002;40:1002. <http://dx.doi.org/10.1029/2000RG000095>.
- Putaud JP, Van Dingenen R, Dell'Acqua A, Raes F, Matta E, Decesari S, et al. Size-segregated aerosol mass closure and chemical composition in Monte Cimone (I) during MINATROC. *Atmos Chem Phys* 2004;4:889–902. <http://dx.doi.org/10.5194/acp-4-889-2004>.
- Reddy K, Phani Kumar DV, Nazeer Ahammed Y, Naja M. Aerosol vertical profiles strongly affect their radiative forcing uncertainties: study by using ground-based lidar and other measurements. *Remote Sens Lett* 2013;4:1018–27. <http://dx.doi.org/10.1080/2150704X.2013.828182>.
- Saha S, Moorthi S, Pan HL, Wu X, Wang J, Nadiga S, et al. Climate forecast system reanalysis. *Bull Am Meteorol Soc* 2010;91:1015–57.
- Sciare J, Oikonomou K, Cachier H, Mihalopoulos N, Andreae MO, Maenhaut W, et al. Aerosol mass closure and reconstruction of the light scattering coefficient over the Eastern Mediterranean Sea during the MINOS Campaign. *Atmos Chem Phys* 2005;5:2253–65. [SRef-ID: 1680-7324/acp/2005-5-2253].
- Seibert P, Frank A. Source-recepto matrix calculation with a Lagrangian particle dispersion model in backward mode. *Atmos Chem Phys* 2004;4:51–63.
- Seinfeld JH, Pandis SN. Atmospheric Chemistry and Physics: From Air Pollution to Climate Change. New York, USA: J. Wiley and Sons; 1998.
- Smirnov A, Holben BN, Eck TF, Dubovik O, Slutsker I. Cloud-screening and quality control algorithms for the AERONET database. *Remote Sens Environ* 2000;73:337–49.
- Stohl A, Hittenberger M, Wotawa G. Validation of the Lagrangian particle dispersion model FLEXPART against large scale tracer experiments. *Atmos Environ* 1998;32:4245–64.
- Stohl A, Forster C, Frank A, Seibert P, Wotawa G. Technical note: the Lagrangian particle dispersion model FLEXPART version 6.2. *Atmos Chem Phys* 2005;5:2461–74.
- Tesche M, Ansmann A, Müller D, Althausen D, Engelmann R, Freudenthaler V, et al. Vertically resolved separation of dust and smoke over Cape Verde using multi-wavelength Raman and polarization lidars during Saharan Mineral Dust Experiment 2008. *J Geophys Res* 2009;114:D13202.
- Theodosi C, Smoliotis D, Zarmpas P, Kocak M, Mihalopoulos N. Carbonaceous aerosols over the Mediterranean and Black Sea. Advances in Meteorology, Climatology and Atmospheric Physics. Springer Atmos Sci 2013;2013:1233–8.

- Torres B, Toledano C, Berjón A, Fuertes D, Molina V, Gonzalez R, et al. Measurements on pointing error and field of view of Cimel-318 Sun photometers in the scope of AERONET-Europe. *Atmos Chem Tech* 2013;6:2207–20.
- Torres B, Dubovik O, Toledano C, Berjón A, Cachorro VE, Lapyonok T, et al. Sensitivity of aerosol retrieval to geometrical configuration of ground-based sun/sky-radiometer observations. *Atmos Chem Phys* 2014;14:847–75.
- Tsekeri A, Amiridis V, Kokkalis P, Basart S, Chaikovsky A, Dubovik O, et al. Application of a synergistic lidar and sunphotometer algorithm for the characterization of a dust event over Athens, Greece. *Br J Environ Clim Chang* 2013;3:531–46.
- Tunved P, Hansson HC, Kerminen VM, Ström J, Dal Maso M, Lihavainen H, et al. High natural aerosol loading over boreal forests. *Science* 2006;312:261–3. <http://dx.doi.org/10.1126/science.1123052>.
- Wagner J, Ansmann A, Wandinger U, Seifert P, Schwarz A, Tesche M, et al. Evaluation of the lidar/radiometer inversion code (LIRIC) to determine microphysical properties of volcanic and desert dust. *Atmos Meas Tech* 2013;6:1707–24.
- Winker DM, Vaughan MA, Omar A, Hu Y, Powell KA, Liu Z, et al. Overview of the CALIPSO mission and CALIOP data processing algorithms. *J Atmos Oceanic Tech* 2009;26: 2310–23. <http://dx.doi.org/10.1175/2009JTECHA1281.1>.
- Yu H, Remer LA, Chin M, Bian H, Tan Q, Yuan T, et al. Aerosols from overseas rival domestic emissions over North America. *Science* 2012;337:566–9. <http://dx.doi.org/10.1126/science.1217576>.